Volume 7 | Number 11 | November 2014 | Pages 3445–3816

Energy & Environmental Science

www.rsc.org/ees

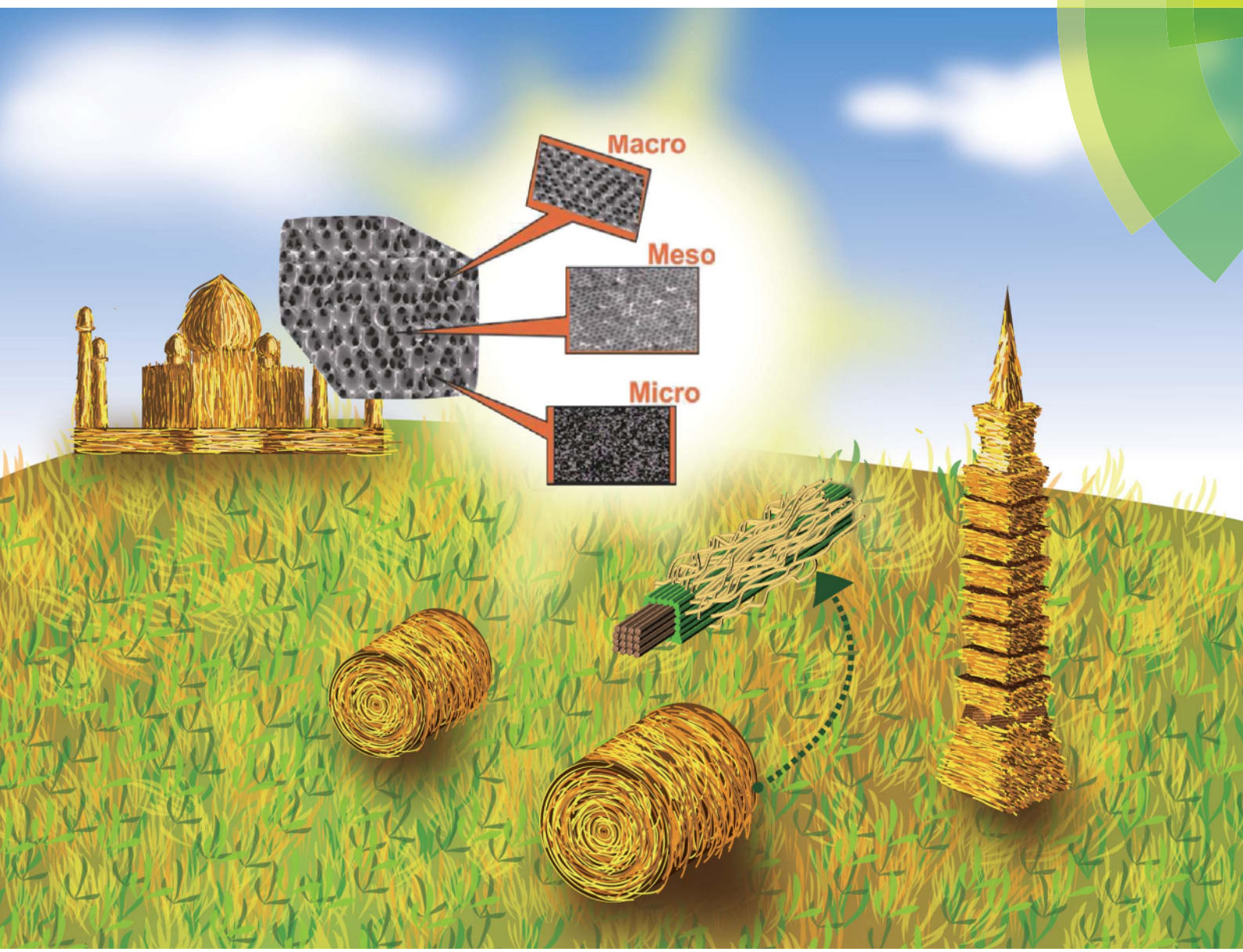

ISSN 1754-5692

ROYAL SOCIETY OF CHEMISTRY

MINIREVIEW

Dutta, Bhaumik and Wu

Hierarchically porous carbon derived from polymers and biomass: effect of interconnected pores on energy applications

Energy & Environmental Science

MINIREVIEW

Cite this: *Energy Environ. Sci.*, 2014, **7**, 3574

Hierarchically porous carbon derived from polymers and biomass: effect of interconnected pores on energy applications

Saikat Dutta,*[a] Asim Bhaumik*[b] and Kevin C.-W. Wu*[a]

Received 4th April 2014
Accepted 29th May 2014

DOI: 10.1039/c4ee01075b

www.rsc.org/ees

Hierarchically porous carbons (HPCs) with 1D to 3D network are attracting vast interest due to their potential technological application profile ranging from electrochemical capacitors, lithium ion batteries, solar cells, hydrogen storage systems, photonic material, fuel cells, sorbent for toxic gas separation and so on. Natural raw-materials such as biomass-biopolymer derived hierarchical nanostructured carbons are especially attractive for their uniform pore dimensions which can be adjustable over a wide range of length scales. Good electrical conductivity, high surface area, and excellent chemical stability are unique physicochemical properties which are responsible for micro/nanostructured porous carbon to be highly trusted candidate for emerging nanotechnologies. This review focuses on the 'out-of-the-box' synthetic techniques capable of deriving HPC with superior application profiles. The article presents the promising scope of accessing HPCs from (1) hard-templating, soft-templating, and non-templating routes, (2) biopolymers with a major focus on non-templating strategies. Subsequently, emerging strategies of hetero-atom doping in porous carbon nanostructures are discussed. The review will highlight the contribution of synergistic effect of macro–meso–micropores on a range of emerging applications such as CO_2 capture, carbon photonic crystal sensors, Li–S batteries, and supercapacitor. Mechanism of ion transport and buffering, electrical double layer enhancement have been discussed in the context of pore structure and shapes. We will also show the differences of HPC and ordered mesoporous carbon (OMC) in terms of their synthesis strategies and choices of template for self-assembly. How the remarkable mechanical strength of the HPCs can be achieved by selecting self-assembling template, whereas collapse of mesostructure *via* decomposition of framework occurs due to poor thermal stability or high N-content of the carbon source will be discussed.

Broader context

The inter-connected pore network in hierarchically porous carbons (HPCs) consisting of macro, meso, and micropores is currently an attractive candidate for advanced technological applications ranging from electrochemical supercapacitors, Li batteries, solar cells, and fuel cells. However, despite the ceaseless development of porous carbons, limited success has been achieved in the synthesis of HPCs by conventional hard-templating methods. Besides, non-renewable carbon sources have been utilized for the fabrication of HPCs. From a long-term perspective, looking for biorenewable carbon sources for HPCs is essential along with developing unconventional non-templating routes that retain the framework of the pore-networks and also offer high specific surface areas and desired pore sizes and shapes. We herein review how polymers, block-copolymers, and biopolymers have been utilized as carbon sources to offer HPCs with versatile nanostructures. Heteroatom doped mesoporous carbon monoliths with hierarchical pores are accessible from N-containing polymeric resins. The derived HPCs demonstrated the synergistic effect of macro-, meso- and microporosity in energy-related applications where ion-transport, buffering, electrical double layer enhancement, and ion diffusion play significant roles. The effect of interconnected pores in CO_2 adsorption and photonic crystal sensors are described. The advantages of HPC over OMC are discussed. The current progress of HPCs derived from biopolymers, challenges, and future applications are critically presented.

1. Introduction

Naturally occurring species are employed as resource for a wide range of materials which suggests that a significant fraction of complex functionalities of living systems are based on their hierarchical structures.[1] Compared to conventional porous materials with uniform pore dimensions that can be adjusted over a wide range of length scales, hierarchical porous materials

[a]*Department of Chemical Engineering, National Taiwan University, Taipei, Taiwan 10617. E-mail: saikatdutta2008@gmail.com; kevinwu@ntu.edu.tw; Tel: +886 33669534*

[b]*Department of Materials Science, Indian Association for the Cultivation of Science, Jadavpur, Kolkata-700032, India. E-mail: msab@iacs.res.in; Fax: +91 33-24732805*

with well-defined pore dimensions and topologies offer minimized diffusive resistance to mass transport by macropores, and high surface area for active site dispersion over the micro- and/or mesopores.[2] Such a novel type of interconnected porous carbon materials with a 1D to 3D network are currently attracting a great degree of interest due to their potential technological application profile ranging from electrochemical capacitors,[3] lithium ion batteries,[4] solar cells,[5] hydrogen storage systems,[6] photonic materials,[7] fuel cells,[8] and sorbents for toxic gas separation.[9] Good electrical conductivity, high surface area, and excellent chemical stability are certain unique physicochemical properties which have caused micro/nanostructured porous carbon to be a highly trusted candidate for emerging nanotechnologies. Novel porous carbon materials with controlled morphology, porosities, and architectures; especially carbon frameworks with hierarchical porosity, namely, mesopores in combination with macropores or micropores; are highly desirable due to their unique structural features compared with carbon materials containing macropores connected with mesopores. The design of hierarchical nanostructured carbons (HNCs) with tailored macropores/mesopores and doping of electron-donating element has emerged as a promising field of further investigation with an extensive scope. The most commonly used synthetic technique for fabrication of HNCs is "nanocasting" (hard templating) with hierarchical nanostructured silica (HNS) as template to impregnate with an appropriate carbon source, followed by carbonization of the composite, and subsequent removal of the template. Primarily, apart from obtaining ordered mesoporous carbons (OMCs) (Fig. 1a),[10] the same with macro/mesoporous arrays, disordered HNCs with macro/mesoporosity, and hollow macroporous core/mesoporous shell were also obtained using a nanocasting strategy.[11]

Major challenges for the fabrication of ordered HNCs with 3D-interconnected macroporous and mesoporous structures

Saikat Dutta obtained his PhD from IISc, Bangalore in 2008. He worked as postdoctoral fellow in Taiwan, India and in the USA. He received a Fulbright Postdoctoral Fellowship in 2012 while working at the Department of Chemistry, University of Florida, USA. After a job as a scientist in India for a short period (2013–2014), he joined Professor Kevin C.-W. Wu's laboratory at the Department of Chemical Engineering, National Taiwan University. Dr Dutta is co-author of more than 30 research publications in scientific journals. His research experience includes chemical and material aspects of biopolymers, energy applications of materials, and enzymatic biofuel production.

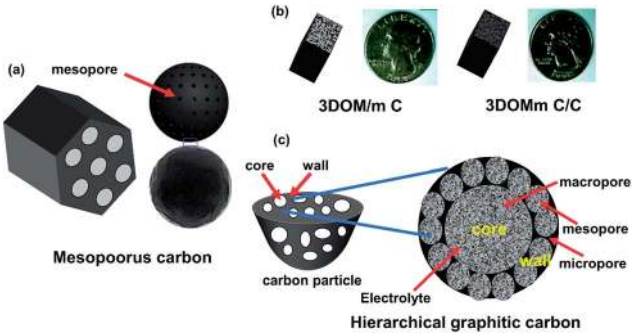

Fig. 1 Schematic representation of (a) 2D mesoporous carbon, (b) three-dimensionally ordered macroporous monolithic carbon (3DOM/m C) and a monolithic carbon–carbon nanocomposites material (3DOM/m C/C); (c) 3D hierarchical porous texture of core, walls, and pores (mesoporous walls, microporous, and macroporous cores) of hierarchically porous graphitic carbon materials.

Professor Asim Bhaumik received his PhD from NCL, Pune in 1997. After postdoctoral research as a JSPS fellow at the University of Tokyo, (1997–1999) and an associate researcher at Toyota Central R&D Labs. Inc., Japan (1999–2001), in 2001 he had joined the faculty in IACS, India. His research focuses on several aspects of energy, environment and biomedical science, including porous materials for adsorption, gas storage, catalysis, sensing, photocatalysis, DSSC and drug delivery applications. He is coauthor of 250 research publications and inventor of 13 patents. He is a board member of several journals and a Fellow of the Royal Society of Chemistry.

Kevin C.-W. Wu is currently an associate professor at the Department of Chemical Engineering, National Taiwan University (NTU), Taiwan. He received his PhD degree from the University of Tokyo, Japan in 2005. He worked on the orientational control of 2D hexagonal mesoporous thin films with Professor Kazuyuki Kuroda (Waseda University, Japan, 2005–2006) and with Professor Victor S.-Y. Lin's group (Iowa State University, USA, 2006–2008) as post-doc. He started his own research group in NTU in August 2008. His current interest is the synthesis of porous nanoparticles and thin films with desired structural orientation and functionalities for biomedical and energy-related applications.

arise from the complexity of interconnected meso/macroporous HNSs with long-range order. Particularly interesting are those nanostructured porous carbon materials[12] or carbon materials exhibiting three-dimensional (3D) hierarchical porous textures (containing pores at different scales, from micropores to mesopores, up to macropores) that combine high specific surface areas with proper channels and allow efficient diffusion of any substance (*e.g.*, analytes, adsorbates, electrolytes *etc.*) to the entire surface of the material.[13] Meso- and macro porosity exert a significant effect in introduction of more graphitic, nitrogen doped carbon into the mesopores of a three-dimensionally ordered macroporous monolithic carbon (3DOM/m C) by chemical vapor deposition to produce a monolithic carbon–carbon nanocomposites material (3DOM/m C/C) (Fig. 1b).[13a] Constructing different nanoscaled pores with interconnections is very important and this greatly depends on the synthetic strategies of the hierarchically porous carbons (HPCs) and the level of the microstructure. To date, well-defined HPCs are accessible *via* hard-/soft-templating approaches and post-activation combined methods. For example, Cheng and co-workers prepared a 3D periodic hierarchical porous graphitic carbon by using alkaline system consisting of $Ni(OH)_2$/NiO-phenolic resin as a hard template (Fig. 1c),[14] and Lu and co-workers described the HPCs obtained by post-activation of a Pluronic F127-templated phenolic resin.[15]

However, most of the templates are expensive and the post-synthetic removal of the template to produce a carbon replica requires additional processing steps that are usually very much time-consuming and harmful for environmental safety. These limitations impart to HPCs an uncompetitive price-to-performance ratio as compared with other materials and thus limit their commercial viability. Obviously, the problem can be fully eliminated with the incorporation of hierarchical porosity by using any auxiliary template. Therefore, building a controllable hierarchical porous structure from a biorenewable source through a template-free method is a big challenge today.

2. Scope

In this review, soft-templating and hard-templating, as well as non-templating, strategies developed for the fabrication of hierarchical porous carbon nanomaterials from various carbon-rich precursors such as polymers, copolymers and biomass-derived polymers as the carbon source are surveyed. The aim of this article is to emphasize the newly explored carbon precursors and naturally occurring biopolymers for their wondrous future prospects in deriving nanostructured HPC materials. Subsequently, a perspective on advanced applications of HPCs for emerging areas of energy storage and generation including reversible CO_2 capture for clean energy technology, carbon photonic crystals, lithium–sulfur batteries, and supercapacitors is provided. The review will mainly focus on the application profiles of the hierarchical porous carbons emphasizing the effect of the interconnectivity of the pore-network on the efficiency of the materials for a specific application. Thus this will help in better understanding of the interconnected-pores–property interrelationship. A comparative description of the synthesis strategies of HPCs and ordered mesoporous carbons (OMCs) is provided which emphasizes the factors responsible for the growth of hierarchical porous nanostructures unlike the nanostructure of OMCs. The article is completed with brief discussion on the applications of HPCs derived from biorenewable sources and relevant conclusions.

3. Fabrication of HPCs from polymers and biomass

3.1. Hard-templating

A large number of techniques have been explored to access HPCs with combined macro- and mesoporosity mainly based on the dual-templating strategy where two templates with dimensions at different length scales are combined to originate multimodal pores.[15,16] Primarily, these strategies involve nanocasting (hard templating) or a combination of hard and soft templates.[17,18] Among other techniques, template replication of hierarchical inorganic materials[13a] and sol–gel[19,20] methods are known. A major challenge to date has been the development of HPCs with very high surface areas, pore volumes and porosities at all three different length scales: macro-, meso-, and micro in a simple material platform. Additional challenges with the synthesis techniques include the requirement to synthesize porous inorganic materials or special nanoparticles as hard templates which involve time-consuming multiple steps and high expense. Furthermore, most of the already explored soft-templates are based on rather expensive and non-renewable surfactants and block-copolymers. Moreover, the size of the mesopores may be difficult to tune due to aggregation of the nanoparticle carbon precursor matrix. Ice templating has been known for its potential for fabricating macroporous and hierarchical nanostructures.[21,22] Based on the dual templating strategy, combined ice templating beside a hard template (colloidal silica) followed by physical activation generates excellent interconnected macro-, meso- and microporosity, respectively as shown by Estevez and co-workers.[23] It is observed that combined silica particles (hard template) and glucose molecules (as carbon source) were expelled away from growing ice crystals (hard template) by plunging the mixture into liquid nitrogen. The glucose–silica composite scaffold offers an interconnected macroporous carbon–silica structure which remains intact during pyrolysis and silica etching (Fig. 2a). Most importantly the resulting HPC scaffold contains macroporous walls made of interconnected mesoporous carbons (Fig. 2b). A distinct advantage is that this approach minimizes the aggregation of hydrophilic silica particles by instantaneous locking within the glucose matrix and subsequent carbonization. The process offers the bimodal nature of mesoporosity observed in the pore size distribution when using silica particles of different size. Moreover, the pore size of the carbon material increases due to the aggregation during freezing. Ice-template–silica-particle derived HPCs have a macro- and mesopores (multimodal) dominated texture with tight control and tenability of their porosity in terms of size and extent. This offers an HPC monolith with desired shape and size along with high pore

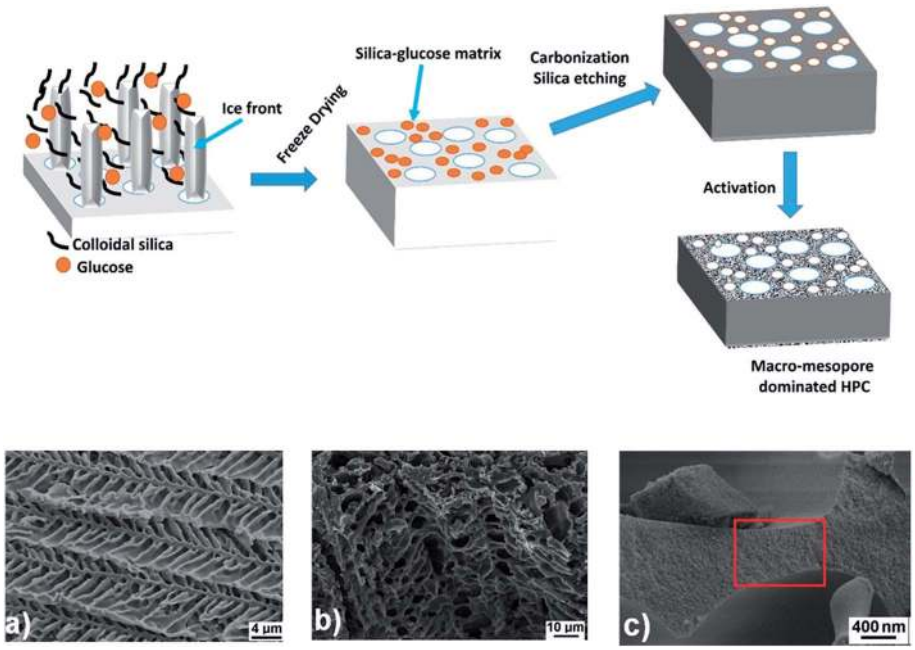

Fig. 2 Ice-templating route to access HPC dominated by macro and mesopores. SEM images: (a) glucose–silica composite; (b) carbonized HPC materials (HRSEM); (c) macroporous walls of the glucose–silica material. ((a)–(c) are reproduced from the ESI of ref. 26 with permission, Copyright, RSC 2013.)

volumes and large pore sizes, making this as excellent candidates for amine based CO_2 capture.

3.2. Soft-templating

Soft-templating can be a good alternative method to access HPCs in which pore structure collapse can be minimized using molecular species in the reaction media, which after gelation, stabilize the pores from collapsing during drying and carbonization.[24] It is proposed that micelles formed during the process act as templates for the construction of pores. HPCs of tunable pore size through soft-templating can be obtained when a cationic polyelectrolyte poly(diallyldimethylammonium) chloride (PDADMAC) is utilized as soft template while using resorcinol–formaldehyde (RF) gel as carbon source.[25] There is an stabilizing effect of the cationic polyelectrolyte on the sol–gel nanostructure in which the porosity of the gel is maintained during the drying process. The introduction of a scaffold for the mass production of HPC monoliths while using triblock copolymer F127 as soft template and phenol–formaldehyde (PF) resin as carbon precursor offers HPCs decorated with micro- and meso-porosity prepared by surface coating and solvent evaporation-induced self-assembly (EISA).[26] In this soft-templating method of transformation of the monolith into the HPC with ordered mesopores through thermo-polymerization, the hierarchical porous architecture is retained while the bulk structure of the scaffold (sugarcane bagasse) was destroyed. This soft-templating method simplifies greatly the production of porous carbon by making it unnecessary to use a complex drying procedure. A dual templating (hard–soft) approach can give rise to HPC with new nanostructure. A flow-enabled self-assembly approach using hierarchically assembled amphiphilic diblock copolymer micelles and inorganic nanoparticles which were crafted over large areas results one-step hierarchical self-organization, *i.e.* parallel threads comprising amphiphilic diblock copolymer micelles and inorganic nanoparticles on the nanometer scale.[27] This type of hierarchical assembly obtained from block copolymer micelles would open up ways to fabricate novel HPCs.

So far, few cases of HPC fabrication using polymers and biomass-derived molecules as the carbon source and hard- or soft-templating strategy have been investigated. Among these, dual templating (hard–soft) have been found more promising for fabricating interconnected porosity. The major hurdle is the efficient fabrication of a hierarchical nanostructured silica or other template with a tailored hierarchical porosity of meso/macropores. An additional difficulty associated with the hard templating process is template removal under concentrated basic conditions. Either decomposition or etching are the strategies to remove the hard template. The removal of any porous inorganic template requires time-consuming multiple steps. At the same time, most of the soft templates used for self-assembly are based on surfactants and block-copolymers, which rather expensive and non-renewable. In some cases, the size of the mesopores can also be difficult to fine-tune because of the aggregation of the nanoparticles in the polymerizing carbon precursor matrix.[27] In addition, soft-templating techniques like sol–gel suffer from the critical drawbacks associated with the long synthesis time required for gelation, solvent exchange and supercritical drying. Further, major difficulties are associated with template removal in the nanocasting and soft-templating methods[28] irrespective of the carbon source; an efficient non-templating approach to access porous carbons with a

controllable pore structure and good mechanical strength is highly desirable. Thus, a self-assembly process of the carbon source without a surfactant in the reaction system is a challenging task.

3.3. Non-templating

The 3D nanoscaled architecture not only provides a continuous electron pathway to ensure good electrical contact, but also facilitates ion transport by shortening diffusion pathways.[29–32] The major challenge for the development of carbon based electrode materials for high-performance energy-storage is how to achieve desirable properties such as large surface area, high conductivity, efficient porosities in the micro-, meso- or macropores, 3D nanoarchitecture and high-level heteroatom-doping. Among the non-template based strategies, a noteworthy approach based on polypyrrole (PPy) microsheets as precursors for carbon and KOH activation offers HPC with hierarchical porous microstructures exhibiting macroporous frameworks, mesoporous walls, and microporous textures. This pore network is ideal for diffusion of the active ions.[33]

In PPy-derived HPCs, mesopores with diameter 10–50 nm were detected in the carbon walls, which are wider as compared to that of the traditional HPCs and activated carbons (pores smaller than 4 nm). This is due to the efficient phase separation between the hydrophobic carbon and water during the KOH activation process. This material also exhibits an annealing-temperature-dependent stability of the pore network. For example, a pore widening maximum of 500 nm at 700 °C was recorded. Among the advantages of HPCs derived from PPy sheet, the most significant is the high surface area that leads to an electrode/electrolyte interface sufficient to form electric double layers. Another advantage is that the hierarchical porous network not only ensures fast ion diffusion by shortening the diffusion pathways, it also utilizes macroporous frameworks as ion-buffering reservoirs, mesoporous walls as ion-highways for fast ion transmission, and microporous textures for charge accommodation. Additionally, these features also provide continuous electron pathways, important for achieving high-rate performance. Non-templating chemical activation methods have also offered porous carbons with micro- (~1.2 nm)[34] and mesoporosity, which are obtained from the hydrothermal carbonization of polysaccharides (starch and cellulose). Bio-resourced carbon can also be derived from yeast, which contains an amorphous matrix and fibrillar network that burns off to deliver carbon material.[35] Here, the fraction of narrower micropore (<0.7 nm) formation depends on the degree of activation of the carbons.

Fabrication of polystyrene-derived HPC (PS-HPC) with a unique hierarchical porous nanonetwork depends on constructing carbonyl cross-linking bridges between PS chains *via* a template-free method.[2,36] Fabrication of spherical HPC by linear polystyrene depends on the construction of carbonyl (–CO–) crosslinking bridges between linear polystyrenes in which carbonyl crosslinking bridges simultaneously provide the resulting hierarchical porous polystyrene (HPP) with a high crosslinking density and sufficient oxygen atoms. This forms a hierarchical pore structure during carbonization.[2–4,37] Introducing an appropriate pre-cross-linking density into polystyrene nanospheres could minimize the chances of the distortion of spherical shapes during the process of swelling and crosslinking. Indeed, $-C_6H_4-$ crosslinking bridges by incorporating divinylbenzene (DVB) ensure the stability of styrene–divinyl benzene (St–DVB) copolymer nanospheres with spherical shape, and result in mesopores of dimension 2–50 nm *via* the compact aggregation of St–DVB nanospheres.[37] This non-templating strategy is quite different from PPy microsheet-derived HPCs which greatly depend on the chemical activation method for 3D hierarchical pore construction. In this process, $-C_6H_4-$ crosslinking bridges provide stability to the nanospheres during swelling and –CO– crosslinking bridges offer good nanostructure inheritability in carbonization. In this process, access to the small sized monodisperse nanoparticles is essential for the fabrication of HPC with mesopores after aggregation of the particles. Dispersion polymerization and delay in addition ensures the formation of smaller nanoparticles (55 nm) by using a low styrene nucleation concentration which further ensures the spherical shape of the St–DVB nanospheres. Carbonyl (–CO–) crosslinking bridges in CCl_4 result in a hierarchical pore network by intra-/inter-sphere crosslinking of the polystyrene chains of the nanospheres (Fig. 3). As a result, the intra-sphere space is subdivided into numerous micropores by the as-constructed intra-sphere crosslinking bridges. The attack of carbocations (CCl_3^+) on the surface of nanospheres, resulting in inter-sphere $-CCl_2-$ crosslinking bridges and stacking of nanospheres in a certain orientation, leads to a 3D network nanostructure containing micropores inside the nanospheres. The formation and growth of network nanoparticles from a template-free method involves the crosslinking of linear polystyrene chains that are hard to control in terms of the shape and size distribution of the particles, which limits the fabrication of HPCs with tunable structures.

A hierarchical porous network of 3D interconnected micro-, meso-, and macropores can also be accessible from the carbonization of an hierarchical porous polyaromatic precursor obtained from aromatic hydrocarbons (AHC) (polynaphthalene, polypyrrole).[38] When the origin of the hierarchical pore network in aggregates of carbon spheres is based on the methylene bridges between phenyl rings, a fast ion transport/diffusion behavior and increased surface area usage in electric double-layer was found. The special nature of these AHC-derived HPCs depends on their micropores in a 3D interconnected network inside the cross-linked AHC microspheres imparting exceptionally high electrochemically accessible surface area for charge accumulation. The method of HPCs obtained through methylene bridges between aromatic rings offers a maximum surface area 455 $m^2\ g^{-1}$ (S_{BET}), which is indeed less than that can be obtained *via* –CO– bridged polystyrene copolymer derived HPCs (S_{BET} 887 $m^2\ g^{-1}$). The total pore volume (max 0.41 $cm^3\ g^{-1}$) of AHC-derived HPC is much less than that of the polystyrene copolymer derived HPCs which indicates the advantages of the introduction of –CO– crosslinking bridges for nanostructure inheritability during carbonization. The superior

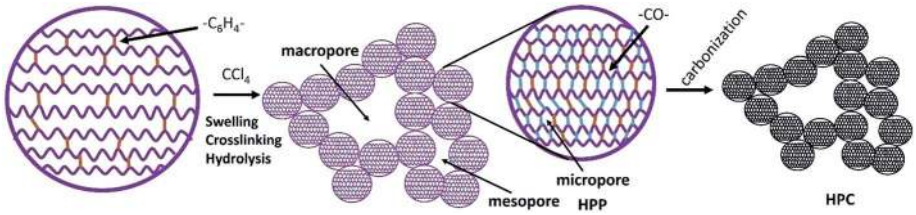

Fig. 3 Mechanism for the formation of hierarchical porous carbon (HPC) by intra-/inter-sphere crosslinking of polystyrene chains of nanospheres *via* a template-free method.

electrical conductivity offered by AHC-derived HPC is perhaps due to the formation of aggregates of spherical carbon spheres composed of turbostratic carbon with a weakly ordered graphitic microstructure which is different from the origin of micropores from direct cabonization or activation processes. Turbostratic carbon[39] is generally a variant of h-graphite, stacked up by graphene layers with regular spacing but different degree of stacking ordering. This weakly ordered graphitic microstructure can enhance the electrical conductivity.

HPCs can be obtained *via* hydrothermal carbonization (HTC) of glucose and fructose as carbon sources, which generally undergo dehydration to 5-hydroxymethylfurfural[40] under HTC conditions, and the resulting polyfuran-type molecules aggregate into secondary spherical particles of the final size. In this non-templated process, poly(ionic liquid)s (PILs) act as a stabilizer of primary nanoparticles formed at the initial stage and allow only growth by further addition of monomers.[42] This occurs by electrostatic repulsion exerted by the PIL to minimize agglomeration by lowering the particle size to <50 nm. From this stage, final hierarchical particle (Fig. 4) forms *via* ordered mesoporous carbons (OMCs) through the use of block copolymers as soft template, typically using resorcinol–formaldehyde resins as the carbon source.[41] The multivalent binding power of PILs has been explored over ILs for the formation of pores apart from its catalytic effect on the HTC process.[42] This reveals that, in the PIL-based HTC process, the macromolecular architecture of PIL and the nature of anion control the formation of HPCs with the desired pore network and functionality.

In order to optimize the structural features of hierarchical porous carbon monoliths (HCMs), an approach of incorporating host foreign components in the macropores, particularly those showing high CO_2 capture capability, would be a novel strategy. The synthesis of such HCM-based composites allows further improvement of their volumetric CO_2 capture ability. A recent study of incorporating metal–organic frameworks into the hierarchical pores of HCMs with a MOF ($Cu_3(BTC)_2$) (BTC = 1,3,5-benzenetricarboxylic acid), known for its promising CO_2 capture ability, was reported (Fig. 5).[43] In HCM–$Cu_3(BTC)_2$

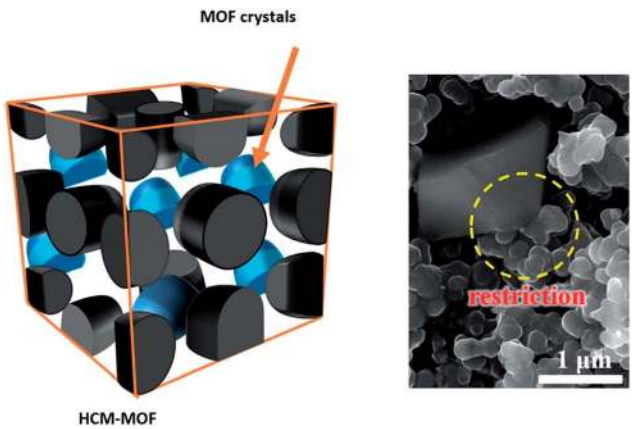

Fig. 5 HPC monolith containing MOF crystallites inside the macropores and an SEM micrograph of HPC–$Cu_3(BTC)_2$. (Figure is reproduced from ref. 35 with permission, Copyright, American Chemical Society, 2012.)

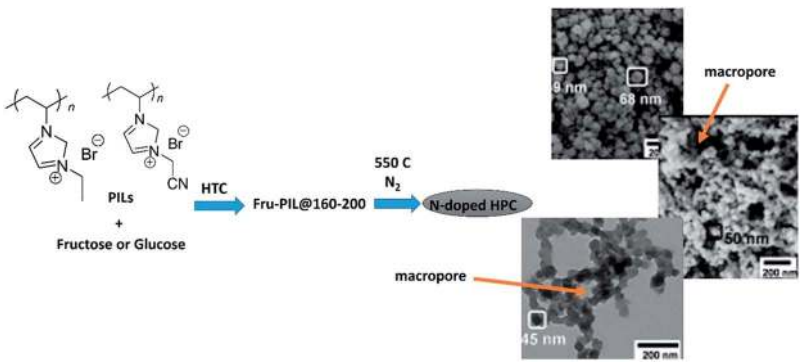

Fig. 4 Hierarchical porous N-doped carbon nanostructure using PILs as a multipurpose agent. (Figure is reproduced from ref. 42 with permission, Copyright Wiley-VCH, 2013.)

composites, macropores of the HCM matrix provide a micro-environment for the growth of $Cu_3(BTC)_2$ crystallites and are dispersed within the HCM matrix involving a restriction effect of the carbon skeleton of the HCM. The HCM's polar surface and high bulk density with incorporation of MOF crystallites in the macropores of HCM provides a novel strategy for practical CO_2 adsorption.

Alkali (KOH or NaOH) treatment is an effective method for activating porous carbon in order to enhance the porous structure and pore widening, which exerts superior electrochemical performance for example with high capacitance and excellent rate capability in both aqueous and non-aqueous electrolytes.[44–46] This method can be more effective for the preparation of hierarchical porous carbon using a non-templating route. A poly(vinyldene fluoride) (PVDF) derived porous carbon can be further improved by a two-step carbonization–activation process in which alkali (NaOH) acts as an interceptor of HF and an activation agent.[47] Such a trick improves the percentage of meso- and macropores in the hierarchical interconnected network. With the increase of the concentration of the NaOH activator, the percentage of meso- and micropores increases and thus the pore volume with thinner pore walls shows a higher activation degree. This results in a very high pore volume of 2.28 $cm^3\ g^{-1}$ and BET surface area of 2711 $m^2\ g^{-1}$. When comparing one-step activation with the two-step by NaOH an improved electrochemical performance is recorded with the one-step activated material, which reveals the efficiency of the former method and is perhaps due to the molten NaOH poured over the fresh surface of the micropores obtained by PVDF pyrolysis making a higher degree of activation with an increase in the abundance of mesopores with a wider distribution in the hierarchical interconnected pore network.

Activation of such polystyrene-derived HPC with KOH can give rise to a unique 3D interconnected large meso- and macroporous structure (27.3 and 68.5 nm, respectively) in the carbon network.[48] The high surface area of KOH-activated PS-HPC (3023 $m^2\ g^{-1}$) is even higher than that of the KOH activated ordered mesoporous carbon (2060 $m^2\ g^{-1}$) but, however, lower than that of the KOH-activated polypyrrole-derived carbons which possess irregularly shaped platelets or particles of larger size (~20 μm).[49] The special nature of these PS-HPC materials is that a large number of micropores and small mesopores whose pore size are large enough for ILs to access are formed within the carbon framework during KOH activation. This provides a large interface for the formation of the electric double layer. An ideal non-templating strategy is therefore using the inexpensive to manufacture and easily sourced carbon; however, limited methods have been reported, which allows a huge scope for the future.

4. Biopolymer derived porous carbon

The application of biomaterials as biological template is known for the nanostructuration of various inorganic materials and metal nanoparticles for which cellulose and polysaccharide nanocrystals play a significant role.[50–52] However, scope of accessible porous materials containing ordered well-defined pores from biomass has not been explored until recently. As a promising renewable resource, biomass offers an attractive raw material, and starch has already been explored for the preparation of hierarchical porous carbons.[53–55] Alginate, a naturally occurring polysaccharide extracted from marine brown algae, has attracted substantial attention for applications in the immobilization of enzymes and proteins and as a template in the fabrication of nanostructured semiconductor materials.[56,57] Alginate has abundant carboxyl and hydroxyl groups in its polymeric carbon matrix and it is particularly convenient as template in the aqueous phase due to the presence of negative charges of the glucoronic and mannuronic units.[58,59] When all these functional groups have been converted to carbon oxides and water, the polymeric carbon matrix can be converted naturally to carbonaceous materials upon carbonization, making alginate a suitable precursor for the fabrication of porous carbons.

The simplest approach to access porous materials from biomass is pyrolysis of native biomaterial under closed conditions or an inert atmosphere. For potential applications like supercapacitors, the uniformity of porosity in biomass would be most advantageous to obtain hierarchical porous carbon nanostructures derived from natural renewable resources, making the strategy highly economical. In such case, the application of homogeneous biopolymer hydrogels or hydrothermal carbonization is essential. In addition to these, understanding the process of formation of hierarchical pore networks in the carbon monolith obtained *via* carbonization is essential. Controlled carbonization of alginic acid fibers, prepared through a simple wet spinning method, offers varied mesopores and micropores with different shapes and sizes around the nanoparticles that construct a hierarchical porous network.[60]

The wet-spinning method offers preservation of the regular and fiber-like shape of the alginic fibers, which can be retained after carbonizing with filaments exhibiting uniform 1D morphology with a diameter ~10 μm. Under higher magnification (Fig. 6a), however, it is clear that the filament is composed of nanosized carbon particles (less than 10 nm) with a porous texture and no homogeneity in pore arrangements. Fig. 6b shows the morphology of a single filament, which exhibits a smooth surface both on the exterior and cross section of the filament under low magnification. Abundant interspaces around the nanoparticles revealed from the TEM image (Fig. 6c) that the carbon fibers are composed of an interconnecting 3D network of carbon particles and form a hierarchical porous structure composed of large mesopores (~19 nm pore diameter) and abundant micropores (<2 nm). However, more essential is to understand the pathways of formation of the hierarchical porous network from a controlled carbonization process of an alginate framework in which oxygen might play a significant role in formation of graphenic carbon atoms; as observed in the pyrolysis of alginate in presence of phosphorous source, which offers a P-doped graphene.[61]

Developing an efficient and facile synthesis protocol using the precursors accessible directly from natural sources for the preparation of 1D nanoporous carbon with well-tailored

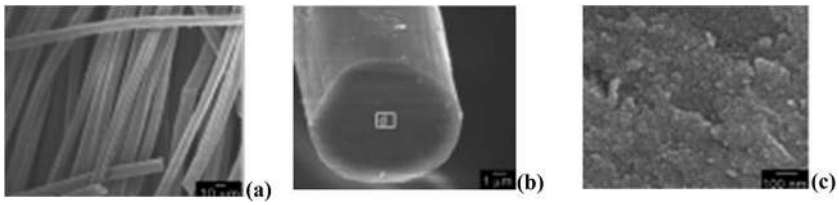

Fig. 6 Typical SEM image of as-prepared HPCFs obtained from alginic acid fibers: (a) regular fiber-like shape of alginic fibers after cabonization; (b) morphology of a single filament with a smooth surface both on the exterior and cross section of the filament; (c) under higher magnification the filament is composed of nanosized carbon particles surrounded by fissures and hillocks with a inhomogeneous porous structure. (Published from the ref. 17 with permission, Copyright Wiley-VCH, 2010.)

architectures would be of great significance. Toward this direction, it is demonstrated that electrospun fiber-like natural cocoon microfibers can be directly transformed into 1D carbon microfibers with an average diameter of 6 μm. The most relevant fundamental question would be how a unique 3D porous network, consisting of 1D carbon microfibers built with numerous carbon nanoparticles (10–40 nm), was obtained *via* carbonization (Fig. 7).[62] The recipe of the network of hierarchical porous structure is that these carbon nanoparticles contain micropores and their compact and loose aggregation leads to the formation of mesopores and macropores, respectively. Interlacing of the 1D carbon microfibers themselves in the carbonized cocoon leads to the formation of large macropore. Due to their effective pore interconnectivity, high surface area and large pore volume, as well as high nitrogen content, the as-prepared 1D HPC microfibers (HPCMF) exhibit superior electrochemical performance as binder-free electrodes for supercapacitors and show promising adsorption behavior for organic vapors.

Biomass-derived porous carbons, such as from fungi,[63] corn grain, lignocellulosic materials,[64] fish scales,[65] starch,[66] celtuce leaves[67] have already been reported. These showed great potential as electrode materials for supercapacitors or as solid adsorbents for CO_2 capture. In such pyrolysis methods, by optimizing the carbonization temperature, the porosity and capacitance of the resulting porous carbon can be balanced. For example, porous activated carbon derived from celtuce leaves (CL) by air-drying and pyrolysis offers a continuous and distorted layered microstructure which can facilitate KOH impregnation and activation (Fig. 8). Indeed nanoscale pores and local curvature were formed in as-prepared carbon due to the KOH etching of CL and generated substantial micro/mesopores of extremely small size (0.5 to 5 nm) and large mesopores and/or textural macropores (30 to 60 nm) that were interconnected and distributed homogeneously throughout the porous structure.

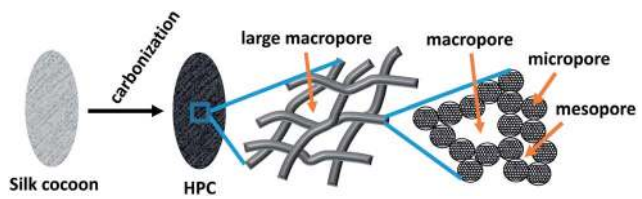

Fig. 7 Silk cocoon as source of hierarchical carbon.

Alkali (KOH or NaOH) treatment can also be used as effective strategy for constructing or improving the hierarchical pore network in biomass-derived porous carbon, as demonstrated for HPC microspheres derived from porous starch.[68] In this case, the KOH activation of the carbon microspheres resulted in a new porous structure on the surface of the ladder-like channel (Fig. 9f). The pores created by KOH along with the macropores inherited from the precursor offer a 3D hierarchical structure with an incredibly high BET surface area of 3251 $m^2 g^{-1}$. Most of the macropores were inherited from the precursor. There are four main regions, including the ultrafine 0.4–0.7 nm and 0.9–1.3 nm micropore region. The 4–14 μm pores in the starch precursor contribute more to the total volume of HPC microspheres. The predominant pore size in HPC microspheres is in the range of 0.7–4 μm which is likely to be due to shrinkage during carbonization.

Natural cellulose substances such as filter paper and cotton possess a macro-to-nanoscopic random morphological hierarchy consisted of β-D-glucose chains. Replication of this sophisticated network at the nanometer level was realized previously by coating ultrathin metal oxide gel films on each cellulose nanofiber surface *via* a surface sol–gel process.[69] Stable suspensions of nanocrystalline cellulose (NCC) can be obtained through hydrolysis of bulk cellulosic material with sulfuric acid. In water, suspensions of NCC organize into a chiral nematic phase that can be preserved upon slow evaporation, thereby resulting in chiral nematic films.[70,71] NCC–silica composite films may also be used to generate mesoporous carbon (MC) with a high specific surface area and excellent chiral nematic organization (Fig. 10).[72] Though soft-templating is a more promising strategy, however, while using NCC as structural template, the use of mesoporous silica is essential for mesoporosity and preservation of the long-range chiral organization. This is due to the formation of linkages between the carbon regions during pyrolysis, which may be prevented without using silica or using higher silica loading and the formation of thicker silica walls. At an optimum silica concentration, maximum BET surface are (1465 $m^2 g^{-1}$) and micropore volume (1.22 $cm^3 g^{-1}$) can be achieved. Chiral nematic mesoporous carbon (CMC) also exhibits locally aligned pores originating from local nematic organization. This CMC film contains smooth surfaces with a repeating layered structure perpendicular to the surface. Apart

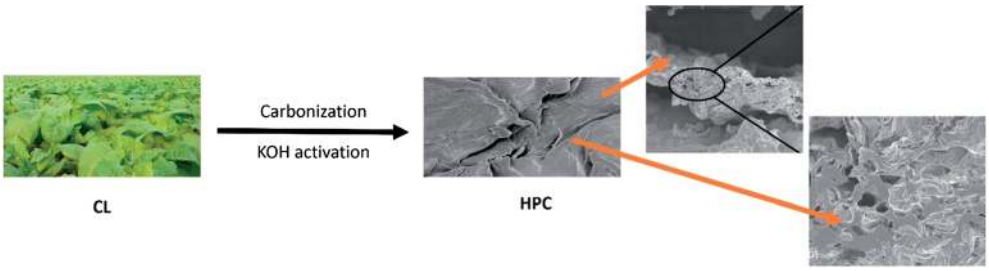

Fig. 8 Carbonated celtuce leaves' surface morphology and cross-section morphology showing the pore network.

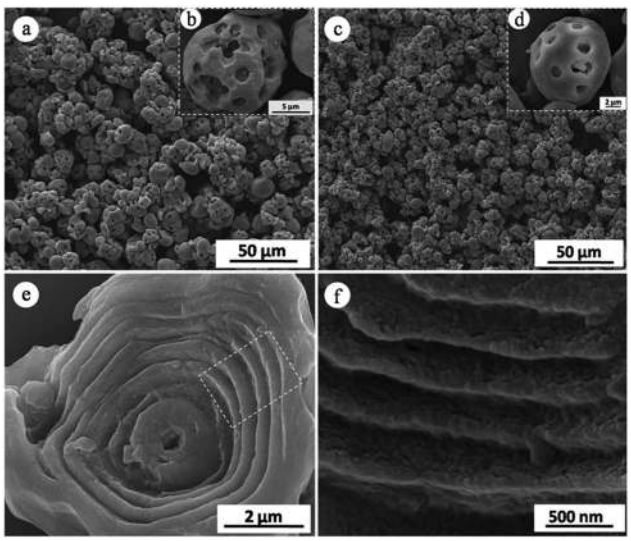

Fig. 9 The SEM images of (a) the porous starch precursor, (b) a porous starch granule under high magnification, (c) the hierarchical porous carbon microspheres, (d) the hierarchical porous carbon microspheres under high magnification, (e) the internal ladder-like microstructure of the hierarchical porous carbon microspheres and (f) the selected part in (e) under high magnification.

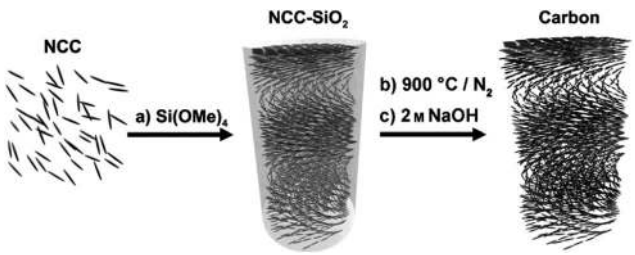

Fig. 10 Chiral nematic porous carbon *via* NCC–silica composite films, pyrolysis at 900 °C, and silica removal from the carbon–silica composite.

from the great possibility of CMC materials as hard-templates capable of transferring chiral nematic structure to the other material, this also displays semiconducting properties which increase with rising temperature.

As a promising nanochemical resource, biomass-derived materials have several advantages. They are naturally abundant and many are extracted industrially on a large scale as low-value waste products; for example, lignin from kraft pulping. Currently, new approaches for utilizing biomass-derived cellulose as a source of HPC and other new materials have been reported, however, in the near future, we hope that both extracted biopolymers and native biomass will be explored.

5. Hetero-atom doped porous carbon monolith

The incorporation of heteroatoms, such as B, N, P and O, into the carbon lattice can enhance significantly the mechanical, semiconducting, field-emission, and electrical properties of carbon materials.[73] These heteroatoms in the porous carbon may enhance the electrical conductivity, influence the wettability, or consequently maximize the electroactive surface area.[74–77] Recent studies suggests that surface functional groups or doped heteroatoms play important roles in improving the performance of the carbon electrodes.[78–80] Doping carbon materials with electron rich atoms has its own advantages for advanced technological applications. Such a strategy becomes ideal when the biomass-derived proteins serve as precursors for synthesizing carbon materials with unique structure, high specific surface area (805.7 $m^2 g^{-1}$), partial graphitization, and very high bulk nitrogen content (10.1 wt%). However, the above method depends on the templating strategy of egg white-derived protein to template the structure of mesoporous cellular foam.[77] Current carbon supercapacitors have extensively used redox reactions to increase their charge-storage capacity. Redox reactions associated with oxygen-containing phenol or quinone/hydroquinones can contribute one electron; phosphorus atoms which stabilize oxygen functional groups during electrochemical charging and gas-phase catalysis. This improves reaction stability and selectivity.[81,82] Boron atoms in a carbon lattice are able to promote the chemisorption of oxygen for a more-reactive carbon surface.[83] The advantage of nitrogen doping to the porous carbon surface causes a shift of the Fermi level to the valence band in the carbon electrode that is essential for supercapacitor applications. The combined effect of nitrogen/oxygen-containing functional groups was also evident in capacitance-enhancement.[74]

Two methods are commonly used to prepare nitrogen-rich carbon materials. One is the simple heat treatment of nitrogen-containing precursors (such as melamine-based polymers,

polyacrylonitrile, vinylpyridine resin, and silk fibroin) under an inert atmosphere.[84–86] The other method is the low-temperature treatment (250–350 °C) of carbon materials in a mixture of ammonia and air with different volume ratios.[87] The location of the N-centers of the carbon lattice of the porous carbon monolith contributes to the efficiency of the materials for supercapacitor and gas adsorption applications. Generally, HPC obtained from the carbonization of nitrogen-containing precursors offers more quaternary nitrogen centers (N-Q) (located at the center and valley position of the carbon lattice) which lack an ammonia-assisted carbonization method. Ammonia-assisted carbonization of thermosetting-type phenolic resin obtained *via* magnesium hydroxide templating offers significant nitrogen doping to carbon, which increases the surface area with the involvement of different nitrogen groups for ion transport and also depends on the relative redox activities of the nitrogen groups.[88] In the case of magnesium hydroxide templating, heat treatment in ammonia results in an unexpected increase of the BET specific surface area and micropore volume. This happens due to edge-nitrogen atoms connected with two carbon atoms, a motif which prevents the growth of the carbon lattice, leaving more space in the form of micropores. The generation of micropores or their expansion occurs due to the release of hydrogens which etch carbons, causing removal of carbon atoms from lattice.

The CO_2 adsorption capacities of nitrogen-rich porous carbons have been less studied as compared with amine-functionalized porous silica. As compared to commercially available activated carbons, polymer-based synthetic porous carbons have high purity, good reproducibility, and well-defined pore structures. Thus, such porous carbons have also been modified to nitrogen-rich porous carbons by deliberate selection of N-containing carbon precursors, such as melamine. For instance, highly nitrogen-enriched porous carbons were prepared from melamine–formaldehyde resins.[89] Recently, various nitrogen-containing porous carbon monoliths were fabricated and used for CO_2 capture and separation.[90] Using resorcinol–formaldehyde as carbon precursors and the amino acid L-lysine as the catalyst, a type of nitrogen-doped porous carbon monolith was synthesized by Lu and co-workers which possesses a maximum CO_2 capture capacity of 3.13 mmol g^{-1} at 25 °C and 1 atm under a flow of pure CO_2.[82,91]Subsequently, a nitrogen-containing porous carbon monolith with fully interconnected macroporosity and mesoporosity was fabricated, which could withstand a pressure of up to 15.6 MPa.[89,91]

To avoid using harsh chemicals for activation and sacrificial templates, physical activation to obtain activated carbon materials is highly desirable from both environmental and economic points of view. The CO_2 uptake capacity can be enhanced by incorporating basic N-functional groups and narrow micropores (<1 nm) with high adsorption potential. Porous activated carbon monoliths (ACMs) can be accessed *via* activation–carbonization of mesoporous polyacrylonitrile (PAN) monoliths in an oxidizing CO_2 environment (Fig. 11).[92] The formation of carbon with a lamellar phase occurred by carbonization of rigid polymer with an extended 2D-framework obtained from the PAN monolith *via* cyclization inside the polymer framework. Cyclization–aromatization imparts extra rigidity to the polymer network which may be responsible for the creation of narrow micropores. During carbonization, removal of nitrogen from the framework causes fusion of the molecular ladders which result in extended sheet-like lamellar carbon frameworks. Micropores randomly distributed all over the skeleton of the microstructures and N-rich porous surface are held responsible for CO_2 uptake with maximum of 11.51 mmol g^{-1} at 273 K.

Phosphate-functionalized carbon materials are interesting because of the widening of the operational voltage window with aqueous electrolytes and the subsequent increase of the energy that can be attained.[93] A resorcinol-based deep-eutectic solvent (DES), composed of resorcinol, choline chloride and glycerol, assisted the synthesis of phosphate-functionalized carbon monoliths (PfCMs) *via* the polycondensation of formaldehyde in the presence of phosphoric acid as catalyst, giving access to a bicontinous porous network built with highly cross-linked clusters that are aggregated and assembled into a stiff, interconnected structure.[94] Bi-continuous (with micropores and mesopores) structures contain macropores of 0.56 μm resulting from the spinodal decomposition process at the resorcinol polycondensation stage in which a polymer-rich phase may form with the segregation of the non-condensed matter. The DES-assisted synthesis offers hierarchical porosity in the phosphate functionalized carbon monolith with direct assembly of carbon cylinders, which are excellent for supercapacitor electrodes. In this process, DES plays multiple roles such as tailoring the textural properties and composition of the resulting carbon materials as a structure directing agent and carbonaceous precursor. Moreover, the template effect of DESs was reflected in HPC monoliths with a maximum pore surface area of 600 m^2 g^{-1} and narrow mesopore diameter distributions.

N and B co-doped carbon monoliths with hierarchical pores can be accessible *via* a self-assembly-carbonization process starting from poly(benzoxazine-*co*-resol) and ionic liquid $[C_{16}mim][BF_4]$ as the carbon and boron sources, respectively.[95] A high skeleton density and fully interconnected pore network with ultramicropores (pore width < 1 nm) was obtained. This pores are suitable for the diffusion of electrolyte ions by minimizing the molecular diffusion limitation, thus potentially advantageous for the enhancement of supercapacitor performance. The nanostructure of the carbon–boron co-doped carbon (CNB) contains a random combination of graphitic and turbostratic stacking with short range ordering and displays a graphite-like microstructure with good electrical conductivity

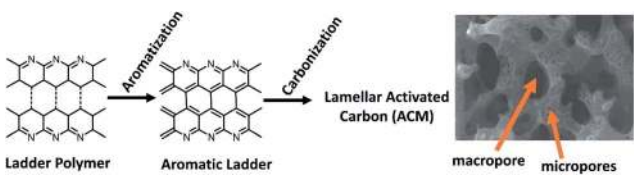

Fig. 11 Formation path of ACMs with narrow micropores in the carbon framework.

due to the multi-length-connected carbon framework. The electron conductivity in the carbon materials is enhanced due to the redistribution of π electrons in the presence of substituted boron and nitrogen that weakens C–C bonds and strengthens C–O bonds when exposed to air. The ionic liquid plays the role of introducing heteroatoms into the carbon framework, through particle involvement in the condensation process.

From the above discussion, it is revealed that for improved conductivity of ions for a range of applications such as supercapacitors, the introduction of heteroatoms to the local graphitic carbon matrix is essential. Multiple heteroatom incorporation into a carbon matrix is a comparatively new strategy to enhance electron conductivity for electrochemical energy storage applications. This strategy depends on the molecular design of monomers and a choice of solvent/media which is capable of supplying heteroatoms to the carbon matrix during the condensation process. Simultaneous control of nanoporosity and electrochemical accessibility of the nitrogen atoms are essential for nitrogen-enriched nanoporous carbons and a general synthetic pathway is desired. However, the most frequently used strategy so far is the use of well-defined block copolymers as precursor for nitrogen-enriched carbon, and the sacrificial block serves as a source of mesoporosity.

6. Synergistic effect of macro–meso–micropores for applications

Compared to conventional porous materials consisting of uniform pore dimensions that can be adjusted over a wide range of length scales, hierarchical porous materials with well-defined pore dimensions and topologies can exhibit minimized diffusive resistance to mass transport from macropores and a high surface area for active site dispersion from micro- and/or mesopores. Depending on the specific requirement of many emerging applications related to energy storage, environmental cleaning, and sensing, a hierarchical nanoarchitecture of the carbon materials is essential. A number of emerging applications of carbon materials is identified and the desired hierarchical interconnecting porous network is discussed.

6.1. CO_2 storage materials

The development of new porous materials as sorbents for CO_2 removal *via* selective adsorption finds potential application in flue gas treatment and natural gas upgrading, which are considered as clean energy technologies. This captured CO_2 can further be used as feedstock to produce liquid fuels or can be offered to microbes that consume CO_2 and produce fuels. Carbon capture and sequestration in the form of CO_2 adsorption is a coherent extension of solar-to-fuel and biomass conversions to biofuels. For the capture of CO_2 from flue gas mixtures, the materials are usually operated under ambient conditions. Thus, gas diffusion properties become the dominant factor which indicates balance among the surface area, pore size and interconnected pore structures. Generally, a highly porous adsorbent when doped with nitrogen,[9] or in monolithic form under relatively mild conditions, would facilitate large-scale application. The reversible absorption/desorption based on the humidity swing is very similar to a green leaf, which displays net CO_2 uptake in sunlight and output in the dark; a functional porous material would act as an "artificial leaf" that is able to capture and release CO_2 in ambient air under dry and wet conditions, respectively.[96] The porous support materials, consisting of immobilized quaternary ammonium cations with hydroxide, bicarbonate, or carbonate counter anions, would be desired materials under dry and humid conditions.[97] Materials with high specific surface areas generally contain a large number of micro- and mesopores, which may decrease the kinetics of absorption and desorption due to diffusional limitations. Additionally, the capillary forces in the micropores can also decrease the sorption rates. It would be highly desirable to obtain porous carbon materials accessible from macroporous polymers for reversible CO_2 capture under ambient air by humidity swing with an improved absorption/desorption kinetics controlled by the hierarchical porous framework. Given that recent studies show that both high porosity and interconnectivity between pores makes best-performing materials, such materials can be obtained *via* sacrificial templating. Functional material of same porosity can be accessible from a suitable carbon source, which retains the structure of the template upon carbonization.

For CO_2 capture and storage, the inclusion of analogues of water soluble amines into the walls of solid porous materials and the construction of nitrogen-rich porous adsorbents provide several advantages as compared with the costly regeneration step in amine-based solution absorption processes. A nitrogen-rich porous carbon with a hierarchical micro/mesoporous structure exhibiting fast adsorption–desorption kinetics is highly desirable.[14] Nitrogen-rich porous carbons open the door for the preparation of highly effective carbonaceous adsorbents for CO_2 capture. The relatively low synthetic cost and easy fabrication, combined with an excellent efficiency of CO_2 adsorption and separation, make nitrogen rich porous carbons highly promising for CO_2-selective adsorption in practical applications. Porphyrin based nitrogen rich porous organic polymers (POPs) are another interesting candidate for CO_2 capture from flue gas.[98] A wide range of POPs can be synthesized through extended aromatic substitution involving the condensation of pyrrole with aromatic dialdehydes in the presence of the Lewis acid $FeCl_3$ under solvothermal conditions. The high surface area and N-rich polymeric network together with porosity facilitates their great capacity for CO_2 capture. It has been observed that ordered 3D-hexagonal mesoporous silica HMS-4 functionalized with vinyl groups at the surface of the mesopores could adsorb 5.5 mmol g^{-1} (24.3 wt%) under 3 bar pressure at 273 K[99] due to its advantages of cage-like pore openings, very high surface area and organic functionalization over related mesoporous silica-based materials.

6.2. Carbon photonic crystals as sensors

It has been observed that glassy carbon nanostructures obtained *via* porous silicon templating function as highly

efficient adsorbents for volatile organics and also act as optical vapor sensors.[7] This photonic properties of the carbon-infiltrated composite pSi film were found to be amended from the Si-based sensor and the sensing strength depended on the porous nature of the surface, containing two different types of mesopores. Upon removal of the Si-template, the porous carbon membrane can be retained when immersed in liquid (methanol, ethanol, hexane, toluene) and this can act as a photonic crystal. From highly porous carbon replicas with extremely high structural fidelity in the silicon template, a carbon nanofiber array can be obtained. This carbon nanofiber material in liquid media would be a better alternative to photonic sensors. A similar material can also be used for adsorption–desorption phenomena. The enhancement of the refractive index of the pore interior to red-shift of the position of the photonic stop band is an essential criterion. Thus, a porous layer of carbon acts as an organic toolkit for the silicon surface since carbon is a superior adsorbent which covers uniformly the Si layer.

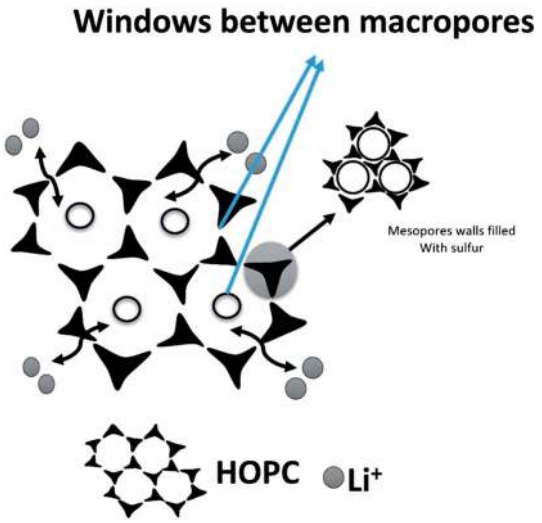

Fig. 12 The electrochemical reaction process inside the pores of the HOPC/S nanocomposite cathode.

6.3. Li–S batteries

Li–S batteries are considered to hold great potential for the next generation of large-scale and high energy density energy-storage devices. In order to tackle the problem of high solubility of intermediate soluble polysulfide ions which results in a shuttle phenomenon between the anode and cathode and a loss of active mass, carbon materials with a hierarchical pore structure can encapsulate and sequester elemental sulfur for high-performance Li–S batteries. This improves electrical conductivity and prevents polysulfide dissolution.[100] It was found that HPCs with mesoporous walls and interconnected macropores encapsulate elements that result in an improvement in the performance of Li–S batteries. The contribution of mesopores in encapsulation of sulfur suggests the presence of an hierarchically ordered structure.[101] This material's walls are composed of spherical mesopores, which indicates a hierarchically ordered porous structure in which elemental sulfur could be impregnated into the mesoporous walls of HPC in a highly dispersed state, which inhibit aggregation of sulfur and initiate essential electrical contact. The mesopores while serving as container, traps elemental sulfur and subsequent lithium polysulfides during the charge–discharge process. In this process, an appropriate ratio of mesopores/macropores facilitates the transition of Li^+ during electrochemical cycling by reducing the ionic and electronic conduction distance. Thus integration of mesopores (sulfur lithiation) and macropores (ion transport) is an essential feature for the next generation of hierarchically porous carbon materials for Li–S battery applications (Fig. 12).

6.4. Supercapacitor

Effective utilization of intermittent renewable sources facilitates energy storage, and electrochemical energy is stored in supercapacitors (SCs) to transport high power within a short period in portable electronic devices and hybrid electric vehicles. The development of an electrode having both a high end specific capacitance is closely related to the availability of interconnected meso-micropores and high rate capability. A hierarchical structure with well-interconnected small and large pores would provide the opportunity to optimize the specific capacitance and rate capability of carbon materials as supercapacitor electrodes. In general, since SCs store energy physically at the electrode/electrolyte interface based on an electrochemical double-layer mechanism for which a high surface area is the basic requirement in carbon-based electrode materials. However, for commercial porous carbon, poor rate performance is usually observed due to the low conductivity, high ion-transport resistance and insufficient ionic diffusion within the tortuous micropores, which limits their application in high-power energy storage devices. What is missing in commercially available carbon is an additional second-order structure of meso/macropores which needs to be induced. Three-dimensional (3D) porous nanostructures are desirable for high-performance electrode materials. The 3D nanoscaled architecture can not only provide a continuous electron pathway to ensure good electrical contact, but also facilitate ion transport by shortening diffusion pathways. The superior electrochemical performance of the carbon is attributed to its unique hierarchical porous structure, which provides the critical features required for advanced supercapacitors: abundant micropores and mesopores provide the electrode with a high accessible surface area, resulting in a large capacitance and high energy density, while interconnected mesopores and macropores facilitate ion transport, which ensure high rate capability and high power density.[102] Hierarchical porous carbon (HPC) materials have elicited porous structures and are able to exhibit the advantages of each pore size with a synergistic effect during the electrochemical charge–discharge process. Macro/mesopores facilitate rapid ion transport by serving as ion-buffering reservoirs and ion-transport pathways,[13d,14] and the micropores enhance the electrical double layer.[103,104] Porous carbon materials, when used as electrodes in electrochemical capacitors, suffer from electrode kinetic problems which are due to the inner-pore ion transport resulting in

poor performance.[103,105] In spite of the fast ion transport ability as well as the high utilization of surface area, HPCs still suffer from a low energy density, a universal bottleneck for electric double-layer capacitors (EDLCs).

6.4.1. Mechanism of ion transport and buffering. The exact mechanism of ion transport within porous materials is highly complex: various factors such as the shape of pores, connectivity, and pore-size distribution should be considered. Apart from the pore structure and shape, nature of electrolyte and solid–liquid interface must all be considered. Among these factors, the inner-pore ion transport resistance and diffusion distance are the most important factors. Generally, micropores ($d < 2$ nm) exhibit large specific surface areas but the pore walls may interfere with ion transportation resulting in poorer power density. When the pore diameters are smaller than solvated ions, the formation of a double layer is supposed to be impossible. However, in certain cases an electric double layer is formed even when the solvated ions are larger than pore diameters when using an organic electrolyte ($LiClO_4$ in propylene carbonate and dimethoxy ethane).[106] In the hierarchical porous structure, electrolyte ions can be delivered smoothly through meso/macropores to micropore surfaces with large specific surface areas. From the fundamental viewpoint, an analysis of the contribution of capacitance by meso/macropores and micropores, separately is essential, however, in the case of porous carbon, pore sizes are continuously distributed from micropores to mesopores, thus making the analysis complicated. In addition, electrolyte transport in their narrow pores causes kinetic polarization and thus the capacitance may be underestimated. It is believed that pores substantially larger than the size of the electrolyte ion and its solvation shell are required for high capacitance. The demonstration of charge storage in pores smaller than the size of solvated electrolyte ions will lead to an enhanced understanding of ionic transport in porous media. These findings should also permit the design of specific supercapacitor applications for longer discharge times where energy density is at a premium, such as in hybrid electric vehicles, where extremely narrow pores should prove optimal, but for pulse power applications, increasing the pore size might be beneficial.

6.4.2. Electrical double layer enhancement. In the case of ordered mesoporous materials, interconnectivity of the channels is beneficial in improving ion diffusion properties. An efficient pore network and interconnectivity of the channels can lead to much lower impedance to ion transport within both the channels and the micropores in the carbon wall, and thus have better electric double layer performance. Doping with an electron deficient element (*e.g.* B) with valance electrons, can introduce a hole charge carrier once it replaces a carbon atom in the carbon lattice. This would increase the charge density and further improve the double layer capacitance. This doping also improves the polarity of a carbon matrix by improving the wettability, and allows an easy diffusion of the electrolyte ions into micropores. The local graphitic heteroatom-incorporated carbon matrix presents a higher conductivity due to their exceptional nanostructure and surface characteristics. According to Largeot *et al.* 2008, when the pore size of the electrode materials is close to the size of an ion in the electrolyte, a maximum capacitance can be obtained.[107] Taking into account the fact that the solvated ion size of K^+ is between 0.36 nm and 0.42 nm, it can be predicted that the pores of these first two regions will contribute the most to the formation of the electric double-layer, leading to a high capacitance as described by Eliad *et al.*[108] The other two regions are the 1.3–3.4 nm micro/mesopore region, which plays a role in electrolyte ion diffusion paths, and the >50 nm macropore region which serves as an ion-buffering reservoir and thus decreases the ion transport distance during electrochemical processes for a starch-derived hierarchical carbon. The contribution of the meso/macro and micropores to C_{DL} can be analyzed by the following equation.

$$C_{DL} = c_{dl,meso}S_{meso} + c_{dl,micro}S_{micro}$$

where $= c_{dl,meso}$ and $c_{dl,micro}$ are the specific electric double layer capacitance of meso/macropores and micropores, respectively. Here the ion sieving effect of micropores comes into play in the case of electrolytes with a positive ion radius slightly larger than the micropore radius.[106]

6.4.3. Ion diffusion. The unique hierarchical porous structure of the HPCs favors the rapid diffusion of electrolyte ions into the pores in supercapacitor electrodes. In a hierarchical porous architecture, large mesopores would provide a fast diffusion channel for the electrolyte and the diffusion distance would also be very short as the micropores are located within the mesopore wall. Micropores are expected to be most efficient in a double-layer formation. The energy and power limitations normally observed at high rate are associated with the complex resistance and the tortuous diffusion pathways within the porous textures. At high discharge current, only some parts of the pores (mainly the outer regions) can be accessed by ions, whereas at low current, both the outer- and the inner-pore surfaces are used for charge storage. The good energy and power performances of HPCs confirm that most of micropores within the mesoporous skeleton can be utilized effectively for charge storage. A reduced capacitance of microporous carbons at large discharging current densities was found; however, such a reduced capacitance also exists for mesoporous carbon materials, probably because of the solute diffusion process.

7. HPC *versus* ordered mesoporous carbon (OMC)

The links between the hierarchically porous structure and their role in performing energy conversion and storage can promote the design of novel nanostructures with advanced properties. Apart from providing large surface areas, HPCs can provide interfacial transport, dispersion of active sites at different length scales of pores (macro, meso, micro), and shorter a diffusion path. Some theoretical calculations predict that the hierarchically macro-, meso-, microporous structured catalysts can reduce the diffusion limitations.[109,110] The low resistance and short diffusion pathway facilitate fast electron and mass transport to enhance the electrochemical energy storage performance.[111] HPCs exhibit outstanding behavior in

diffusion-assisted adsorption applications driven by the different ranges of interconnected pores. This is very different from the ordered mesoporous network which provides shorter diffusion pathways along the carbon particles, and enhances the diffusivity of molecules and/or ions. Generally, while the construction process of HPCs, removal of hard-templates and carbonization of the carbon source material results in microporosity in the resulting carbon and mesoporous network, generated as a result of incomplete pore filling of the hard template.

Ordered mesoporous carbons (OMC) have received considerable attention owing to their large surface area, tunable pore structure, uniform and adjustable pore size, mechanical stability and good conductivity. In spite of these outstanding features, most of the mesoporous carbons derived so far have a highly hydrophobic surface and a limited number of specific active sites, which impedes their practical application. The synthesis of HPC and OMCs depends on several factors such the choice of C-containing precursor or N source for N-doped porous carbons. For example, direct self-assembly of organic–organic amphiphilic block copolymers has been a versatile route to access OMCs, however these strategy suffers from inferior pore structure with poor thermal stability or low N content. The reason behind the collapse of the mesostructure is the pluoronic surfactant with high oxygen content which promotes decomposition of the N-containing part of the precursor. In addition, pyrolysis at high temperature can also accelerate the decomposition of the frameworks, resulting in a collapsed mesostructure. When a direct synthesis of ordered mesoporous carbons from organic–organic self-assembly with a high level of doped element (*e.g.* N) suffers from high N content and large surface area, this is a great challenge and in most cases direct carbonization offers material with a wide pore size and disordered mesostructure.[112]

Hao *et al.* reported the direct self-assembly of poly(benzoxazine-*co*-resol) followed by a carbonization process, obtaining N-doped porous carbons with well-defined hierarchical porosities[90] that contained defined multiple-length-scale pore structures (macro-, meso-, and micropores) of fully interconnected macroporosity and mesoporosity with cubic *Im3m* symmetry. This offers a remarkable mechanical strength to the material. The generation of highly interconnected pores in the nanostructures is dependent on the self-assembly of poly(benzoxazine-*co*-resol) and the carbonization process. In this process, polybenzoxazine segments form hydrogen bonds (Ar–O–H···O) with the EO segment of F127 to a significant extent, which guide the mesostructure assembly within polymer species and the amphiphilic copolymer template (F127). During the following curing step, the unreacted resorcinol and formaldehyde copolymerize with polybenzoxazine. In this case, both the polybenzoxazine and poly(resorcinol-formaldehyde) together form the hybrid skeletons which lead to the formation of stable mesostructures.

In the case of OMCs the N source is external, while for thermosetting polymerization the N source is incorporated. However, in the case of using polybenzoxazine-*co*-resol self-assembly in the presence of F127, the N source is attached to the copolymer, undergoing self-assembly before carbonization. The difference is that resorcinol–dicyandiamide obtains an ordered mesoporous framework and a porous framework with an interconnected multi-length-scale pore structure *via* a copolymer self-assembly is obtained when using polybenzoxazine-*co*-resol. Control experiments revealed that mesopores were generated *via* the assembly of polybenzoxazine and the ethylene oxide (EO) segment of F127 due to the oxygen affinity of the O centers. This reveals that the presence of surfactant F127 is essential for mesopore formation. Further, the condensation of the resorcinol with polybenzoxazine and assembly of the resorcinol segment of the poly(benzoxazine-*co*-resol) with the EO segment offers hierarchical pore formation. When using a resol-based copolymer such as poly(benzoxazine-*co*-resol) with F127 as template, two segments (benzoxazine and resol) interact separately with F127's EO segment *via* H-bonding and electrostatic interactions, and this more complex self-assembly forms in solution, which upon evaporation of solvent and pyrolysis produces inter-connected pore networks in the nanostructure (Fig. 13).[112] This comparative study on the synthesis of OMC and HPCs reveals that the carbon source polymer played a crucial role in determining the nanostructure of the porous carbon when using the same polymer template with oxygen containing blocks.

Ordered mesoporous structures are slightly degenerated, as revealed from the small-angle X-ray direction (SAXS) patterns of the *P6m* 2D hexagonal mesostructure of H-NMC obtained with various mass ratio of dicyandiamide (DCDA) to resol. In this material, uniform mesopores are periodically aligned over a large domain as revealed from cross-sectional field-emission scanning electron microscope (FESEM) analysis.[113]

Unique nanoscale spherical OMCs with extremely high bimodal porosities are an attractive material for applications involving rapid charge–discharge capacity and good recyclability. A two-step nanocasting process to obtain a spherical mesoporous carbon nanoparticle with hierarchical pores involves the application of a silica inverse opal which was used as template for a triconstituent precursor solution containing resol, tetraethylorthosilicate (TEOS) and Pluronic F127 as structure directing agent.[114] This process involves carbonization and etching of the silica inverse opal template, and results in OMC with hierarchical porosity. In this case, silica inverse opal templating creates OMC with a high inner pore volume (2.32 $cm^3\ g^{-1}$), a very high surface area (2445 $m^2\ g^{-1}$) and a bimodal pore size distribution with large and small mesopores of 6 nm and 3.1 nm. This bimodal distribution arises from the porous walls formed by etching the silica from the carbon–silica nanocomposite walls.

8. Future potentials of HPCs in emerging nanotechnologies

The hierarchical pore arrangement of HPCs has placed them far ahead other conventional porous materials for tackling the energy related problems based on their high specific surface area, thermal stability, mass productivity, and fast adsorption–

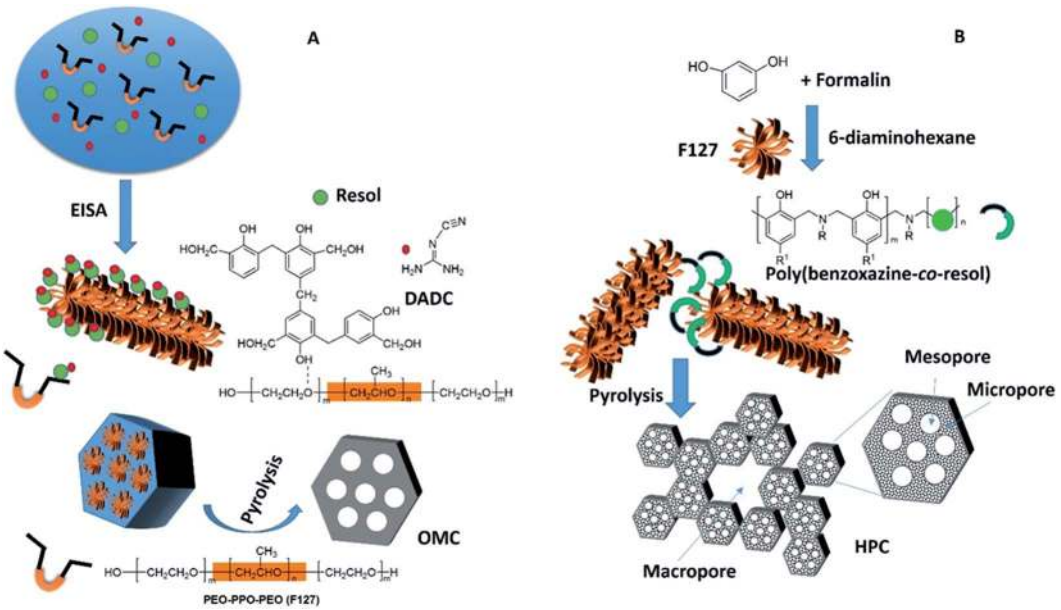

Fig. 13 Formation of HPC and OMC using F127 as soft-templates, where resol and resol-based block copolymer are used as the carbon sources.

desorption kinetics. The possibility of utilizing HPCs derived from a wide range of biomass sources has yet to be employed for next generation technological applications relevant to energy solutions; for example, applications of HPCs in unitized regenerative fuel cells (URFCs), energy-storage systems for uninterrupted power supplies, solar-powered aircraft, and satellites. The bioresourced highly-reproducible 3D morphology with macro-to-mesoporous architecture can resemble the intricate structure of the source. Chemical tailoring of such hierarchically-porous, carbon converted, biogenic structures is envisaged to result in a high degree of enzyme loading for rapid enzymatic applications. Such carbon structure can also be amplified with carboxylic groups by chemical modification and metal deposition, opening the scope for new applications. Several hydrolase enzymes can be attached to the carboxy-functionalized HPCs *via* electrostatic attachment and depending on the loading of enzyme, several biocatalytic process can be derived.

HPC coating on other hierarchically structured materials, especially magnetic materials with a carbon-coated surface with a nanostructured interior, can be suitable candidate for Li-ion batteries due to their unique carbon shell. However such materials open significant scope for energy storage applications in other devices as well. Apart from exploring HPCs for application in storing and generation of energy, HPCs are also promising candidates for the design of catalysts required for selective biomass conversion processes. Highly uniform and conformal coatings on both surfaces and to infiltrate HPCs derived from biomass will have immense significance. Highly dispersed organic and inorganic species on high surface area materials with complex topology are another emerging area, where atomic layer deposition can also be used as alternate method for preparing composites with HPCs.

The enhancement of the energy density of supercapacitors depends greatly on optimized porosity or hybrid devices by employing pseudocapacitive elements. The effect of the low charge carrier density of carbon on the total material capacitance is not considered attentively. It considered that the increase in density of states (DOS) of low density of charge carriers in carbon materials leads to a substantial increase in capacitance as the electrode potential increases.[115] A significant tool would be to improve the carbon capacitor performance, doping with highly graphitic carbons for a stronger degree of electrochemical doping and high skeleton density that may result in enhancement of capacitance.

These apart, HPC would find potential applications in the area of enhancement of photocatalytic applications based on hierarchically organized porous structures which might result in a slow-photon effect and this photonic structural property of HPCs is yet to be explored for solar thermal storage and artificial photosynthesis. A highly opened-up surface structure and hierarchical order would offer a framework with properties of accelerating charge collection and separation,[116] thus a soft–photocatalytic interface favoring mass transfer may be accessible.

Accessing highly ordered DNA nanowires which are used in waveguides, photodetection, nanophotonic switches, logic devices, *etc.* is an attractive field. Controlled evaporation-induced self-assembly of a DNA aqueous solution on the HPC surface may offer aligned DNA nanowires, however the process would depend on the control of flow within the evaporating solution.[117] Such controlled evaporation self-assembly would be remarkable and introduce a new avenue for crafting DNA-based HPC nanostructures for these applications. Further, hierarchical micro/mesopores in an HPC can act as drug-loaded nanocontainers to enhance the targeting capability to tumor

tissues *in vitro* and inhibit tumor growth with minimal side effects *in vivo*.[118]

9. Conclusions

Several energy and environmental solutions require the advancement of highly stable, ordered porous nanostructured materials to enhance the performance of core devices, for purposes such as solar and chemical energy storage, separation of gas molecules, and pollutant removal from air. Particularly, there is a surge in demand for cutting down the emission-levels of CO_2 from nonrenewable sources. The short-term goals of carbon capture and sequestration require the absorptive removal of CO_2 from air. Control and optimization of pore geometry, size, volume, surface area and intrinsic basicity at the surface are crucial to achieve efficient CO_2 capture at pre- and post-combustion power stations. High surface area and ultra-high total pore volume are significantly desired for enhanced applications of hierarchically porous materials. Given their rich properties, HPCs are potential candidates for further pore optimization/functionalization for energy storage, especially as super-capacitor electrode materials, methane storage systems, and Li-ion adsorption–desorption in batteries. Obviously, the selection of a precursor plays a critical role in obtaining desirable porosities in the sp^2-bonded graphenic carbons[119] and N-doping can considerably enhance their CSS application through favorable dipolar interaction with the CO_2 molecules.

In spite of recent advances on the control of the porosity of carbon materials through mainly hard templating (nanocasting) procedures, and the development of novel carbon materials (graphene, carbon nanotubes), porous carbons with an inter-connected pore hierarchy would be the choice for the construction of new generation electrodes for commercial supercapacitors and other energy related applications. To comply with future energy demands, higher control over the textural properties (pore size, volume, and aspect ratio) must be maximized to improve power densities, making them suitable for medium to long-term solutions. Furthermore, it is essential to reduce the cost of accessing carbon materials by exploring precursors such as biomass, which is low-cost, readily available and renewable, thus will play a key role for various purposes. Strategies for deriving hetero-atom doped carbon from biopolymers and their further application as electrodes for use in alkaline supercapacitors depends on the controlled ammonia assisted carbonization when starting from a biopolymer without N-content. Strategies of deriving doped-hierarchically porous carbon from biopolymers can also be developed for other elements such P, B *etc. Ex situ* electrochemical spectroscopy can be used to investigate the evolution of N-functional groups on the surface of the N-doped carbon electrodes in the supercapacitor cell.

The major difficulty faced in constructing interconnected pores in the macro–meso–microporous carbon system from a non-templating route or from a biorenewable source is controlling the pyrolysis step. A dual templating strategy has been evolved for the construction of a hierarchical pore network for crystalline TiO_2 films[120] for application in photoelectrochemical water-splitting due to structural homogeneity and integrity. Consequently, such strategies to access HPC materials from biopolymers have not yet been developed. However, HPCs have not yet been exploited for asymmetric supercapacitors (ASCs) with a faradaic electrode as the energy source and a capacitive electrode as a power source, in which an effective approach to increase the cell voltage has plenty of scope. Additionally, potential raw materials like bacterial cellulose have yet to be explored for the design of HPCs with a network of pores, either as a template or precursor for carbon.

Acknowledgements

SD and KCW Wu thank the Ministry of Science and Technology (MOST), Taiwan (101-2628-E-002-015-MY3, 101-2623-E-002-005-ET, 101-2923-E-002-012-MY3, 103-2811-E-002-018 and 103-2218-E-002-101), National Taiwan University (101R7842 and 102R7740), and the Center of Strategic Materials Alliance for Research and Technology (SMART Center) of National Taiwan University (102R104100) for funding supports. AB wishes to thank GITA, New Delhi for funding through India-Taiwan S&T Cooperation Program.

References

1 J. Aizenberg, J. C. Weaver, M. S. Thanawala, V. C. Sundar, D. E. Morse and P. Fatzl, *Science*, 2005, **309**, 275.
2 C. Zou, D. C. Wu, M. Z. Li, Q. C. Zeng, F. Xu, Z. Y. Huang and R. W. Fu, *J. Mater. Chem.*, 2010, **20**, 731.
3 B.-Z. Fang, J.-H. Kim, M.-S. Kim, A. Bonakdarpour, A. Lam, D. Wilkinson and J.-S. Yu, *J. Mater. Chem.*, 2012, **22**, 19031.
4 H. L. Wang, Y. Yang, Y. Y. Liang, J. T. Robinson, Y. G. Li, A. Jackson, Y. Cui and H. J. Dai, *Nano Lett.*, 2011, **11**, 2644.
5 B.-Z. Fang, M.-W. Kim, S.-Q. Fan, J.-H. Kim, D. Wilkinson, J.-J. Ko and J.-S. Yu, *J. Mater. Chem.*, 2011, **21**, 8742.
6 B.-Z. Fang, J.-H. Kim, M.-S. Kim and J.-S. Yu, *Langmuir*, 2008, **24**, 12068.
7 T. L. Kelly, T. Gao and M. J. Sailor, *Adv. Mater.*, 2011, **23**, 1776.
8 B.-Z. Fang, J.-H. Kim, M.-S. Kim and J.-S. Yu, *Chem. Mater.*, 2009, **21**, 789.
9 P.-Z. Li and Y. Zhao, *Chem.–Asian J.*, 2013, **8**, 1680.
10 J. Liu, T. Yang, D.-W. Wang, G. Q. Lu, D. Zhao and S. Z. Qiao, *Nat. Commun.*, 2013, **4**, 2798.
11 B. Fang, J. H. Kim, M.-S. Kim and J.-S. Yu, *Acc. Chem. Res.*, 2013, **46**, 1397.
12 (*a*) S.-W. Woo, K. Dokko, H. Nakano and K. Kanamura, *J. Mater. Chem.*, 2008, **18**, 1674; (*b*) C. Liang, K. Hong, G. A. Guiochon, J. W. Mays and S. Dai, *Angew. Chem., Int. Ed.*, 2004, **43**, 5785; (*c*) Y. Meng, D. Gu, F. Zhang, Y. Shi, H. Yang, Z. Li, C. Yu, B. Tu and D. Zhao, *Angew. Chem., Int. Ed.*, 2005, **44**, 7053.
13 (*a*) Z.-Y. Wang, F. Li, N. S. Ergang and A. Stein, *Chem. Mater.*, 2006, **18**, 5543; (*b*) L.-Z. Fan, Y.-S. Hu, J. Maier, P. Adelhelm, B. Smarsly and M. Antonietti, *Adv. Funct. Mater.*, 2007, **17**, 3083; (*c*) M. C. Gutierrez, F. Pic, F. Rubio, J. M. Amarilla, F. J. Palomares, M. L. Ferrer,

F. Del Monte and J. M. Rojo, *J. Mater. Chem.*, 2009, **19**, 1236; (*d*) D. Carriazo, F. Pic, M. C. Gutierrez, F. Rubio, J. M. Rojo and F. Del Monte, *J. Mater. Chem.*, 2010, **20**, 773; (*e*) H.-J. Liu, X.-M. Wang, W.-J. Cui, Y.-Q. Dou, D.-Y. Zhao and Y.-Y. Xia, *J. Mater. Chem.*, 2010, **20**, 4223.
14 D. W. Wang, F. Li, M. Liu, G. Q. Lu and H. M. Cheng, *Angew. Chem., Int. Ed.*, 2008, **47**, 373.
15 A. H. Lu, G. P. Hao, Q. Sun, X. Q. Zhang and W. C. Li, *Macromol. Chem. Phys.*, 2012, **213**, 1107.
16 H. Nishihara and T. Kyotani, *Adv. Mater.*, 2012, **24**, 4473.
17 Y. Deng, C. Liu, T. Yu, F. Liu, F. Zhang, Y. Wan, L. Zhang, C. Wang, B. Tu, P. A. Webley, H. Wang and D. Zhao, *Chem. Mater.*, 2007, **19**, 3271.
18 Z. Wang and A. Stein, *Chem. Mater.*, 2008, **20**, 1029.
19 J. Biener, M. Stadermann, M. Suss, M. A. Worsley, M. M. Biener, K. A. Rose and T. F. Baumann, *Energy Environ. Sci.*, 2011, **4**, 656.
20 S. L. Candelaria, R. Chen, Y. H. Jeong and G. Cao, *Energy Environ. Sci.*, 2012, **5**, 5619.
21 L. Estevez, A. Kelarakis, Q. Gong, E. H. Da'as and E. P. Giannelis, *J. Am. Chem. Soc.*, 2011, **133**, 6122.
22 M. C. Gutiérrez, M. Jobbágy, N. Rapún, M. L. Ferrer and F. Del Monte, *Adv. Mater.*, 2006, **18**, 1137.
23 L. Estevez, R. Dua, N. Bhandari, A. Ramanujapuram, P. Wang and E. P. Giannelis, *Energy Environ. Sci.*, 2013, **6**, 1785.
24 Y. Xia, Z. Yang and R. Mokaya, *Nanoscale*, 2010, **2**, 639.
25 J. Balach, L. Tamnorini, K. Sapag, D. F. Acevedo and C. A. Barbero, *Colloids Surf., A*, 2012, **415**, 343.
26 C.-H. Huang and R.-A. Doong, *Microporous Mesoporous Mater.*, 2012, **147**, 47–52.
27 S. Han and T. Hyeon, *Chem. Commun.*, 1999, 1955.
28 N. Pal and A. Bhaumik, *Adv. Colloid Interface Sci.*, 2013, **189–190**, 21–41.
29 Z. Li, L. Zhang, B. S. Amirkhiz, X. Tan, Z. Xu, H. Wang, B. C. Olsen, C. M. B. Holt and D. Mitlin, *Adv. Energy Mater.*, 2012, **2**, 431.
30 B. G. Choi, M. Yang, W. H. Hong, J. W. Choi and Y. S. Huh, *ACS Nano*, 2012, **6**, 4020.
31 H. Jiang, P. S. Lee and C. Li, *Energy Environ. Sci.*, 2013, **6**, 41.
32 L. Qie, W. Chen, H. Xu, X. Xiong, Y. Jiang, F. Zou, X. Hu, Y. Xin, Z. Zhang and Y. Huang, *Energy Environ. Sci.*, 2013, **6**, 2497.
33 B. Li, W. Han, B. Jiang and Z. Lin, *ACS Nano*, 2014, **8**, 2936.
34 M. Sevilla and A. B. Fuertes, *Energy Environ. Sci.*, 2011, **4**, 1765.
35 W. Shen, Y. He, S. Zhang, J. Li and W. Fan, *ChemSusChem*, 2012, **5**, 1274.
36 D. Wu, C. M. Hui, H. Dong, J. Pietrasik, H. J. Ryu, Z. Li, M. Zhong, H. He, E. K. Kim and M. Jaroniec, *Macromolecules*, 2011, **44**, 5846.
37 Q. Zeng, D. Wu, C. Zou, F. Xu, R. Fu, Z. Li, Y. Liang and D. Su, *Chem. Commun.*, 2010, **46**, 5927.
38 X. Huang, S. Kim, M. S. Heo, J. E. Kim, H. Suh and I. Kim, *Langmuir*, 2013, **29**, 12266.
39 Z. Q. Li, C. J. Lu, Z. P. Xia, Y. Zhou and Z. Luo, *Carbon*, 2007, **45**, 1686.
40 (*a*) S. Dutta, *RSC Adv.*, 2012, **2**, 12575; (*b*) S. Dutta, S. De and B. Saha, *ChemPlusChem*, 2012, **77**, 259.
41 (*a*) Y. Huang, H. Cai, D. Feng, D. Gu, Y. Deng, B. Tu, H. Wang, P. A. Webley and D. Zhao, *Chem. Commun.*, 2008, 2641; (*b*) M. C. Gutierrez, F. Pico, F. Rubio, M. Amarilla, F. J. Palomares, M. L. Ferrer, F. Del Monte and J. M. Rojo, *J. Mater. Chem.*, 2009, **19**, 1236.
42 P. Zhang, J. Yuan, T.-P. Fellinger, M. Antonietti, H. Li and Y. Wang, *Angew. Chem., Int. Ed.*, 2013, **52**, 6028.
43 D. Qian, C. Lei, G.-P. Hao, W.-C. Li and A.-H. Lu, *ACS Appl. Mater. Interfaces*, 2012, **4**, 6125.
44 J. Wang and S. Kaskel, *J. Mater. Chem.*, 2012, **22**, 23710.
45 X. He, R. Li, J. Qiu, K. Xie, P. Ling, M. Yu, X. Zhang and M. Zheng, *Carbon*, 2012, **50**, 4911.
46 B. Xu, S. Hou, G. Cao, F. Wu and Y. Yang, *J. Mater. Chem.*, 2012, **22**, 19088.
47 B. Xu, S. Hou, G. Cao, M. Chu and Y. Yang, *RSC Adv.*, 2013, **3**, 17500.
48 H. Zhong, F. Xu, Z. Li, R. Fu and D. Wu, *Nanoscale*, 2013, **5**, 4678.
49 L. Wei, M. Sevilla, A. B. Fuertes, R. Mokaya and G. Yushin, *Adv. Funct. Mater.*, 2012, **22**, 827.
50 N. Lin, J. Huang and A. Dufrense, *Nanoscale*, 2012, **4**, 3274.
51 S. J. Eichhorn, *Soft Matter*, 2011, **7**, 303.
52 K. E. Shopsowitz, H. Qi, W. Y. Hamad and M. J. MacLachlan, *Nature*, 2010, **468**, 422.
53 (*a*) E. Raymundo-Pinero, F. Lerous and F. Beguin, *Adv. Mater.*, 1877, **2006**, 18; (*b*) S. H. Guo, J. H. Peng, W. Li, K. B. Yang, L. B. Zhang, S. M. Zhang and H. Y. Xia, *Appl. Surf. Sci.*, 2009, **255**, 8443.
54 F. Zhang, K. X. Wang, G. D. Li and J. S. Chen, *Electrochem. Commun.*, 2009, **11**, 130.
55 W. Z. Shen, Z. F. Qin, H. G. Wang, Y. H. Liu, Q. J. Guo and Y. L. Zhang, *Colloids Surf., A*, 2008, **316**, 313.
56 S. Dutta, A. K. Patra, S. De, A. Bhaumik and B. Saha, *ACS Appl. Mater. Interfaces*, 2012, **4**, 1560.
57 M. Buaki-Sogo, M. Serra, A. Primo, M. Alvaro and H. Garcia, *ChemCatChem*, 2013, **5**, 513.
58 M. Chtchigrovsky, Y. Lin, K. Ouchaou, M. Chaumontet, M. Robitzer, F. Quignard and F. Taran, *Chem. Mater.*, 2012, **24**, 1505.
59 A. Primo, M. Liebel and F. Quignard, *Chem. Mater.*, 2009, **21**, 621.
60 X. L. Wu, L.-L. Chen, S. Xin, Y.-X. Yin, Y.-G. Guo, Q.-S. Kong and Y.-Z. Xia, *ChemSusChem*, 2010, **3**, 703.
61 M. Latorre-Sanchez, A. Primo and H. Garcia, *Angew. Chem., Int. Ed.*, 2013, **52**, 11813.
62 Y. Liang, D. Wu and R. Fu, *Sci. Rep.*, 2013, **3**, 1119.
63 H. Zhu, X. L. Wang, F. Yang and X. R. Yang, *Adv. Mater.*, 2011, **23**, 2745.
64 F. C. Wu, R. L. Tseng, C. C. Hu and C. C. Wang, *J. Power Sources*, 2004, **138**, 351.
65 W. X. Chen, H. Zhang, Y. Q. Huang and W. K. Wang, *J. Mater. Chem.*, 2010, **20**, 4773.
66 L. Wei, M. Sevilla, A. B. Fuertesm, R. Mokaya and G. Yushin, *Adv. Energy Mater.*, 2011, **1**, 356.

67 R. Wang, P. Wang, X. Yan, J. Land, C. Peng and Q. Xue, *ACS Appl. Mater. Interfaces*, 2012, **4**, 5800.
68 S.-H. Du, L.-Q. Wang, X.-T. Fu, M.-M. Chen and C.-Y. Wang, *Bioresour. Technol.*, 2013, **139**, 406.
69 J. Huang and T. J. Kunitake, *J. Am. Chem. Soc.*, 2003, **125**, 11834.
70 J. Pan, W. Y. Hamad and S. K. Strauss, *Macromolecules*, 2010, **43**, 3851.
71 J. F. Revol, L. Godbout and D. G. Gray, *J. Pulp Pap. Sci.*, 1998, **24**, 146.
72 K. E. Shopsowitz, W. Y. Hamad and M. J. MacLachlan, *Angew. Chem., Int. Ed.*, 2011, **50**, 10991.
73 (*a*) A. Y. Liu and M. L. Cohen, *Science*, 1989, **245**, 841; (*b*) Y. D. Xia and R. Mokaya, *Adv. Mater.*, 2004, **16**, 1553.
74 D. Hulicova-Jurcakova, M. Seredych, G. Q. Lu and T. J. Bandosz, *Adv. Funct. Mater.*, 2009, **19**, 438.
75 L. F. Chen, X. D. Zhang, H. W. Liang, M. Kong, Q. F. Guan, P. Chen, Z. Y. Wu and S. H. Yu, *ACS Nano*, 2012, **6**, 7092.
76 M. Zhong, E. K. Kim, J. P. McGann, S.-E. Chun, J. F. Whitacre, M. Jaroniec, K. Matyjaszewski and T. Kowalewski, *J. Am. Chem. Soc.*, 2012, **134**, 14846.
77 Z. Li, Z. Xu, X. Tan, H. Wang, C. M. B. Holt, T. Stephenson, B. C. Olsen and D. Mitlin, *Energy Environ. Sci.*, 2013, **6**, 871.
78 Z. Wen, X. Wang, S. Mao, Z. Bo, H. Kim, S. Cui, G. Lu, X. Feng and J. Chen, *Adv. Mater.*, 2012, **24**, 5610.
79 H. R. Byon, B. M. Gallant, S. W. Lee and Y. Shao-Horn, *Adv. Funct. Mater.*, 2013, **23**, 1037.
80 Y. Mao, H. Duan, B. Xu, L. Zhang, Y. Hu, C. Zhao, Z. Wang, L. Chen and Y. Yang, *Energy Environ. Sci.*, 2012, **5**, 7950.
81 D. Hulicova-Jurcakova, A. M. Puziy, O. I. Poddubnaya, F. Surez-Garcia, J. M. D. Tascn and G. Q. Lu, *J. Am. Chem. Soc.*, 2009, **131**, 5026.
82 J. Zhang, X. Liu, R. Blume, A. H. Zhang, R. Schlogl and D. S. Su, *Science*, 2008, **322**, 73.
83 D. W. Wang, F. Li, Z. G. Chen, G. Q. Lu and H. M. Cheng, *Chem. Mater.*, 2008, **20**, 7195.
84 D. Hulicova, J. Yamashita, Y. Soneda, H. Hatori and M. Kodama, *Chem. Mater.*, 2005, **17**, 1241.
85 C. O. Ania, V. Khomenko, E. Raymundo-Pinero, J. B. Parra and F. Beguin, *Adv. Funct. Mater.*, 2007, **17**, 1828.
86 Y. J. Kim, Y. Abe, T. Yanaglura, K. C. Park, M. Shimizu, T. Iwazaki, S. Nakagawa, M. Endo and M. S. Dresselhaus, *Carbon*, 2007, **45**, 2116.
87 K. Jurewicz, K. Babel, R. Pietrzak, S. Delpeux and H. Wachowska, *Carbon*, 2006, **44**, 2368.
88 D.-W. Wang, F. Li, L.-C. Yin, X. Lu, Z.-G. Chen, I. R. Gentle, G.-Q. Lu and H.-M. Cheng, *Chem.–Eur. J.*, 2012, **18**, 5345.
89 (*a*) L. Meng and X. Junmin, *J. Phys. Chem. C*, 2014, **118**, 2507; (*b*) C. Ma, J. Shi, Y. Song, D. Zhang, X. Zhai, M. Zhong, Q. Guo and L. Liu, *Int. J. Hydrogen Energy*, 2012, **7**, 7587.
90 G.-P. Hao, W.-C. Li, D. Qian, G.-H. Wang, W.-P. Zhang, T. Zhang, A.-Q. Wang, F. Schuth, H.-J. Bongard and A.-H. Lu, *J. Am. Chem. Soc.*, 2011, **133**, 11378.
91 G.-P. Hao, W.-C. Li, D. Qian and A.-H. Lu, *Adv. Mater.*, 2010, **22**, 853.
92 M. Nandi, K. Okada, A. Dutta, A. Bhaumik, J. Maruyama, D. Derks and H. Uyama, *Chem. Commun.*, 2012, **48**, 10283.
93 D. Carriazo, M. C. Gutierrez, F. Pico, J. M. Rojo, J. L. G. Fierro, M. L. Ferrer and F. Del Monte, *ChemSusChem*, 2012, **5**, 1405.
94 D. Carriazo, M. C. Gutierrez, M. L. Ferrer and F. Del Monte, *Chem. Mater.*, 2010, **22**, 6146.
95 D.-C. Guo, J. Mi, G.-P. Hao, W. Dong, G. Xiong, W.-C. Li and A.-H. Lu, *Energy Environ. Sci.*, 2013, **6**, 652.
96 T. Wang, K. S. Lackner and A. Wright, *Environ. Sci. Technol.*, 2011, **45**, 6670.
97 H. He, W. Li, M. Zhong, D. Konkolewicz, D. Wu, K. Yaccato, T. Rappold, G. Sugar, N. E. David and K. Matyjaszewski, *Energy Environ. Sci.*, 2013, **6**, 488.
98 A. Modak, M. Nandi, J. Mondal and A. Bhaumik, *Chem. Commun.*, 2012, **48**, 248.
99 A. Dutta, M. Nandi, M. Sasidharan and A. Bhaumik, *ChemPhysChem*, 2012, **13**, 3218–3222.
100 X. L. Ji, K. T. Lee and L. F. Nazar, *Nat. Mater.*, 2009, **8**, 500.
101 B. Ding, C. Yuan, L. Shen, G. Xu, P. Ni and X. Zhang, *Chem.–Eur. J.*, 2013, **19**, 1013.
102 Z. Chen, J. Wen, C. Yan, L. Rice, H. Sohn, M. Shen, M. Cai, B. Dunn and Y. Lu, *Adv. Energy Mater.*, 2011, **1**, 551.
103 J. Chmiola, G. Yushin, Y. Gogotsi, C. Portet, P. Simon and P. L. Taberna, *Science*, 2006, **313**, 1760.
104 W. Xing, C. Huang, S. Zhuo, X. Yuan, G. Wang, D. Hulicova-Jurcakova, Z. Yan and G. Lu, *Carbon*, 2009, **47**, 1715.
105 W. Xing, C. C. Huang, S. P. Zhuo and X. Yuan, *Langmuir*, 2009, **25**, 7783.
106 H. Yamada, I. Moriguchi and T. Kudo, *J. Power Sources*, 2008, **175**, 651.
107 C. Largeot, C. Portet, J. Chmiola, P. L. Taberna, Y. Gogotsi and P. Simon, *J. Am. Chem. Soc.*, 2008, **130**, 2730.
108 L. Eliad, G. Salitra, A. Soffer and D. Aurbach, *J. Phys. Chem. B*, 2001, **105**, 6880.
109 G. Wang, E. Johannessen, C. R. Kleijn, S. W. de Leeuw and M.-O. Coppens, *Chem. Eng. Sci.*, 2007, **62**, 5110.
110 G. Wang and M.-O. Coppens, *Chem. Eng. Sci.*, 2010, **65**, 2344.
111 Y. H. Deng, C. Liu, T. Yu, F. Liu, F. Q. Zhang, Y. Wan, L. Zhang, C. Wang, B. Tu, P. A. Webley, H. Wang and D. Zhao, *Chem. Mater.*, 2007, **19**, 3271.
112 (*a*) J. S. Lee, X. Q. Wang, H. M. Luo, G. A. Baker and S. Dai, *J. Am. Chem. Soc.*, 2009, **131**, 4596; (*b*) X. Q. Wang and S. Dai, *Angew. Chem., Int. Ed.*, 2010, **49**, 6664; (*c*) W. Yang, T. P. Fellinger and M. Antonietti, *J. Am. Chem. Soc.*, 2011, **133**, 206; (*d*) J. S. Lee, X. Q. Wang, H. M. Luo and S. Dai, *Adv. Mater.*, 2010, **22**, 1004.
113 J. Wei, D. Zhou, Z. Sun, Y. Deng, Y. Xia and D. Zhao, *Adv. Funct. Mater.*, 2013, **23**, 2322.
114 J. Schuster, G. He, B. Mandlmeier, T. Yim, K. T. Lee, T. Bein and L. F. Nazar, *Angew. Chem., Int. Ed.*, 2012, **51**, 3591.
115 P. Ganesh, P. R. C. Kent and V. Mochalin, *J. Appl. Phys.*, 2011, **110**, 073506.
116 J. Zhang, J. Sun, K. Maeda, K. Domen, P. Liu, M. Antonietti, X. Fu and X. Wang, *Energy Environ. Sci.*, 2011, **4**, 675.

117 B. Li, W. Han, M. Byun, L. Ahu, Q. Zou and Z. Lin, *ACS Nano*, 2013, **7**, 4326.
118 Z. Luo, X. W. Ding, Y. Hu, S. J. Wu, Y. Xiang, Y. F. Zeng, B. L. Zhang, H. Yan, H. C. Zhang, L. L. Zhu, J. J. Liu, J. H. Li, K. Y. Cai and Y. L. Zhao, *ACS Nano*, 2013, **7**, 10271–10284.
119 G. Srinivas, V. Krungleviciute, Z.-X. Guo and T. Yildirim, *Energy Environ. Sci.*, 2014, **7**, 335.
120 R. Zhang, D. Shen, M. Xu, D. Feng, W. Li, G. Zheng, R. Che, A. A. Elzatahry and D. Zhao, *Adv. Energy Mater.*, 2014, **4**, DOI: 10.1002/aenm.201301725.